A Cough Aerosol Simulator for the Study of Disease Transmission by Human Cough-Generated Aerosols

William G. Lindsley,* Jeffrey S. Reynolds,* Jonathan V. Szalajda,** John D. Noti,* and Donald H. Beezhold*

*National Institute for Occupational Safety and Health, Health Effects Laboratory Division, 1095 Willowdale Road, Morgantown, WV 26505

**National Institute for Occupational Safety and Health, National Personal Protective Technology Laboratory, 626 Cochrans Mill Road, Pittsburgh, PA 15236

Corresponding author: Dr. William G. Lindsley
National Institute for Occupational Safety and Health
1095 Willowdale Road, M/S 4020
Morgantown, WV 26505-2845
Phone: (304) 285-6336
Fax: (304) 285-6394
Email: wlindsley@cdc.gov

Running title: Cough aerosol simulator

Abstract

Aerosol particles expelled during human coughs are a potential pathway for infectious disease transmission. However, the importance of airborne transmission is unclear for many diseases. To better understand the role of cough aerosol particles in the spread of disease and the efficacy of different types of protective measures, we constructed a cough aerosol simulator that produces a human-like cough in a controlled environment. The simulated cough has a 4.2 liter volume and is based on coughs recorded from influenza patients. In one configuration, the simulator produces a cough aerosol containing particles from 0.1 to 100 µm in diameter with a volume median diameter (VMD) of 8.5 µm and a geometric standard deviation (GSD) of 2.9. In a second configuration, the cough aerosol has a size range of 0.1 to 30 µm, a VMD of 3.4 µm and a GSD of 2.3. The total aerosol volume expelled during each cough is 68 µl. By generating a controlled and reproducible artificial cough, the simulator allows us to test different ventilation, disinfection and personal protection scenarios. The system can be used with live pathogens, including influenza virus, which allows isolation precautions used in the healthcare field to be tested without risk of exposure for workers or patients. The information gained from tests with the simulator will help to better understand the transmission of infectious diseases, develop improved techniques for infection control, and improve safety for healthcare workers and patients.

Introduction

Acute respiratory tract infections occur more frequently than any other type of illness in humans (Monto 2002). Many of these diseases are thought to be spread in part by infectious aerosols produced when sick individuals cough, sneeze, speak, or breathe (Roy and Milton 2004; Sattar and Ijaz 2002). Unfortunately, identifying the transmission routes of diseases can be quite difficult, especially in the case of airborne transmission, because diseases often use multiple pathways for infection and confounding factors can make it impossible to determine exactly how a particular individual became infected (Hall 2007; Roy and Milton 2004). As a result, controlled studies in a well-defined

environment are needed to better understand the complex processes involved in the spread of potentially infectious aerosols.

Cough-generated aerosols are of particular concern in disease transmission because coughing is a common symptom of respiratory infections and because the violent expulsion of air during a cough generates aerosol particles that can travel two meters or more away from an infected person (Tang et al. 2011; Zhu et al. 2006). Several studies have shown that people expel aerosol particles containing potentially infectious microorganisms during coughing, speaking, or breathing (Fabian et al. 2008; Fennelly et al. 2012; Lindsley et al. 2010; Morawska et al. 2009; Stelzer-Braid et al. 2009), but the dispersion of cough aerosols into the environment and their capacity for spreading microorganisms are not well understood (Morawska 2006). In addition, the relative importance of respiratory aerosols in the transmission of illness is often unclear and disputed (Goldmann 2001; Musher 2003; Tellier 2009). This is especially true for influenza, which is of great concern because of its ability to cause global pandemics with high rates of illness and death. Influenza is thought to spread by person-to-person transfer of mucus (directly or via fomites such as door handles and telephones), by large ballistic spray drops that land on mucous membranes, and by the inhalation of airborne virus-laden particles (Weber and Stilianakis 2008). However, the relative importance of these routes, and of airborne transmission in particular, is debated (Brankston et al. 2007; Tellier 2009; Weber and Stilianakis 2008).

A cough is typically characterized by inhalation to a high lung volume, closure of the glottis, an increase in intrathoracic pressure, a sudden opening of the glottis, and a high initial peak in outward air flow followed by a gradual decrease (Gupta et al. 2009; McCool 2006). After exiting the mouth, the cough air flow forms a jet that gradually widens and then dissipates (Chao et al. 2009; Tang et al. 2009; VanSciver et al. 2011). During coughs, large amounts of aerosol particles from the respiratory tract can be carried into the environment. The aerosols produced during coughing and sneezing are reported to cover a broad size range, usually spanning the detection limits of the

measurement technique used, and the amount of aerosol produced varies greatly from person to person (Gralton et al. 2011; Nicas et al. 2005).

The sizes of cough-generated aerosol particles have a substantial impact on their behavior. Current infection control guidelines distinguish between “droplet precautions”, which are needed for diseases thought to spread primarily by larger spray droplets, and “airborne precautions”, needed for diseases that spread via small aerosols (Siegel et al. 2007). Large droplets (greater than ~50 µm) are primarily affected by gravity; they follow a ballistic trajectory and impact on surfaces or fall onto surfaces within a meter of the source. Intermediate-sized droplets (~10 to 50 µm) can deposit by impaction but can also be carried further from the source by the cough air flow and can travel two meters or more before settling. Small droplets (less than ~10 µm) are much less prone to impaction or settling; they can remain airborne for an extended time and be spread throughout a room by air currents, especially after drying (CDC 2006).

To assist in studying the spread of cough aerosols in the environment, some researchers have built cough aerosol simulators of various types. Simulators make it possible to generate and study these aerosol clouds in a controlled environment and examine the impact of different ventilation systems, disinfection methods, and protective equipment. To et al. (2009) injected a burst of aerosol particles into an aircraft cabin mockup and found that coughing could propel the particles to seats located well forward of their origin. Wan et al. (2007) sprayed droplets into a hospital ward and showed that, while large droplets settled quickly, smaller ones were able to stay airborne for an extended time. Pantelic et al. (2009) used a coughing aerosol simulator to test a personalized ventilation system and found that the system offered partial protection, but that cough aerosols were still able to penetrate through it. Hui et al. (2012) studied the dispersion of small aerosol particles from a human patient simulator during coughing and found that forward dispersion was reduced and lateral dispersion increased by the use of surgical masks and N95 respirators.

The dissemination of diseases by respiratory aerosols is of particular concern to the healthcare community because of the possibility of transmitting illnesses on to other patients and to the workers, who are much more likely to be exposed to these bioaerosols than the general public. For this reason, the U.S. National Institute for Occupational Safety and Health (NIOSH) has been studying airborne infectious diseases and the effectiveness of various type of personal protective equipment (PPE) against them, with a primary focus on influenza. As a part of this effort, NIOSH has built a mechanical cough aerosol simulation system capable of generating an infectious aerosol comparable to that seen in humans and expelling it into a sealed environmental chamber. The original version of this system was used to study the dispersion of cough aerosol in a room and the survival of influenza virus under different environmental conditions (Lindsley et al. 2012; Noti et al. 2013; Noti et al. 2012). The second generation of this cough aerosol simulator, designed to produce a larger cough volume and a much broader size range of aerosol particles, has recently been constructed and tested. The purpose of this report is to explain the design of the system and how it performs and to convey some of the lessons learned during its use.

Materials and Methods

A schematic of the cough aerosol simulator is shown in Figure 1. A computer-controlled linear motor (Model STA2506, Copley Controls) is used to drive a stainless-steel bellows with a 15 cm inner diameter and 33 cm maximum length (#750-600-7-EE, Standard Bellows Company) to produce the air flow of the cough. Two aerosol generators can be used with the system, an air brush (Model 200, Badger Air-Brush Co.) and a micropump nebulizer (Aeroneb AG-AL7000SM, Aerogen). The fluid used for aerosol generation in these experiments was a cell culture medium used to propagate influenza virus (Complete Dulbecco's Modified Eagle Medium (CDMEM) consisting of Dulbecco's Modified Eagle Medium, 100 U/ml penicillin G, 100 µg/ml streptomycin, 2 mM L-glutamine, 0.2% bovine serum albumin, and 25 mM HEPES buffer; all culture reagents were from Gibco). When the micropump nebulizer is used, 8.5 liters/min of dry diluent

air are mixed with the aerosol. The air brush emits about 8.4 liters/min of air at the operating pressure (138 kPa, 20 psi) and no diluent air is added. The air brush, or nebulizer, is attached to a chamber made of standard 2-inch PVC plumbing fittings and is mounted on the top of the bellows assembly. The chamber is 73 cm (29 inches) long to allow the aerosol spray from the air brush to dissipate into the PVC chamber without excessive losses onto the walls. The chamber outlet mouth has a 21 mm inner diameter and an area of 341 cm^2, which is comparable to the mouth opening areas measured during coughs by adult human subjects (Gupta et al. 2009).

The cough aerosol simulator is controlled with a custom computer program written using LabVIEW (National Instruments Corporation). A typical cough sequence goes as follows: The bellows is first moved up to the highest position to empty it as much as possible. The aerosol generator is then activated, along with a vacuum scavenger that draws 20 liters/min of air in from a port near the mouth of the cough simulator to prevent any aerosol from escaping before the cough. The bellows is then slowly moved downward to allow it to become loaded with the test aerosol (this takes about 31 seconds). The bellows then pauses for 3 seconds, the aerosol generator and vacuum scavenger are turned off, and the cough is triggered. During the cough, the linear motor pushes the bellows upward to produce the desired air flow rate and propel the cough aerosol out of the mouth of the simulator. For most of our experiments, the coughing simulator was synchronized with a breathing simulator such that the cough is initiated at the start of an inhalation cycle by the breathing simulator. After coughing, the system waits 6 seconds for the cough to disperse and then moves the bellows downward. When the system is not engaged in a cough sequence, the bellows is held in a position midway between the highest and lowest positions to minimize the motor current required to maintain its position in order to minimize heating of the motor.

Measurements of the air volume and flow rate from the cough simulator were made using an ultrasonic spirometer (Easy-on PC, NDD Medical Technologies, Inc.). Aerosol concentration measurements were performed using a spray droplet size analyzer

(Spraytec Analyzer with an Inhalation Cell, Malvern Instruments Ltd.) equipped with a 300-mm lens, giving it a nominal size range of 0.1 to 900 µm. During our experiments, a large peak in aerosol concentration was typically seen at around 3 to 10 µm, and a second smaller peak was displayed at around 500 µm. After further study and a discussion with the manufacturer, we concluded that this second peak represented noise rather than actual droplets. For this reason, any data for particles larger than 215 µm were discarded during our analysis. It also should be noted that the Spraytec instrument measures aerosol particle volume, not particle count, and thus the manufacturer recommends that the count distribution derived from the volume distribution be regarded as an estimate only.

Results

Cough flow rate. The cough simulator was developed to simulate the dispersion of a potentially infectious cough aerosol from a patient with a respiratory infection. In a previous study, the flow rates and volumes of three voluntary coughs from each of 47 human subjects with influenza were measured (Lindsley et al. 2010). For the present study, in order to determine an appropriate cough volume and flow rate for the system, these coughs were sorted by cough volume into quartiles, and the highest quartile was analyzed to provide a representative "worst-case" cough. These coughs had a mean cough volume of 4.15 liters (standard deviation (SD) 0.51). Similarly, the mean peak flow rate of the highest quartile was found to be 10.5 liters/second (SD 1.1). Human coughs have a consistent general pattern in that the flow rate rapidly reaches a peak value early in the cough and then falls off more slowly. However, because of variations in the timing of the flow peak during different coughs, the cough flow profiles for the different coughs could not be averaged without distorting the profile. For this reason, the patient cough flow profile closest to the mean volume and peak flow rate was selected as the representative cough to be used with the simulator. The representative cough profile had a volume of 4.16 liters and peak flow rate of 11.1 liters/second. A lognormal curve was fitted to the cough profile using this equation:

$$F(t) = V \frac{1}{\sqrt{2\pi}\, t \ln(G)} e^{-\frac{1}{2}\left(\frac{\ln(t)-\ln(M)}{\ln(G)}\right)^2}$$

F(t) is the flow rate in liters/second, V is the total volume of the cough in liters, t is the time in seconds, M is the geometric mean of the curve, and G is the geometric standard deviation. The best fit to the patient cough was found by using V = 4.68, M = 0.293, and G = 2.62, giving a correlation coefficient of 0.904. This equation was then used as a starting point to determine the rate of displacement of the bellows needed to reproduce the patient cough (a 41.4 mm compression of the bellows displaces 1 liter of air). After several trials, the cough simulator was found to provide a good reproduction of the patient cough when using V = 4.68, M = 0.27 and G = 3.00 (Figure 2). Using these parameters, the cough simulator produced a cough volume of 4.2 liters and a peak flow of 11.4 liters/sec, which are very similar to the values for the original patient cough.

Cough aerosol output using an air brush. The particle-size distribution based on the total volume of the aerosol particles in each size bin is shown in Figure 3. The average distribution has a volume median diameter (VMD) of 8.46 µm and a geometric standard deviation (GSD) of 2.86. The average total aerosol volume expelled during each cough was 68.3 µl (SD 3.7). Since the aerosol particles were measured at the mouth of the simulator, this distribution represents the particle diameters and volumes before the aerosol entered the room and began to dry. The count-based aerosol-size distribution has a count median diameter (CMD) of 0.194 µm and a GSD of 1.73 (Figure 4). Figure 5 shows the aerosol concentration in microliters of aerosol per liter of air over the course of a cough. The concentration peaks early in the cough and then falls and levels off during the remainder.

Cough aerosol output using a nebulizer. To help examine the effects of aerosol particle size on the dissemination of cough aerosols, a second configuration of the cough simulator was developed using a micropump nebulizer to generate the test aerosol rather than an air brush. As can be seen in Figure 6, the volume-based particle-size distribution was somewhat smaller than that seen with the air brush, with a VMD of

3.39 µm and a GSD of 2.32. The average total aerosol volume expelled during each cough when using the nebulizer was also 68.3 µl but with a higher standard deviation (SD 10.8). The count-based distribution using the nebulizer had a CMD of 0.185 µm and a GSD of 1.75 (Figure 7). As with the air brush, the aerosol concentration peaks early in the cough and then falls and levels off during the remainder; however, the peak is higher relative to the later part of the cough (Figure 8).

Discussion

The primary motivation for building the cough simulator was to study the role of airborne particles emitted by infected people in the transmission of the influenza virus. The cough aerosol simulator was designed to conduct experiments on the dispersion of cough aerosols in a simulated medical examination room, the survival of microorganisms contained in the aerosol particles, and the effectiveness of protective measures. Our design is the first cough aerosol simulator for which the air flow and aerosol output have been well characterized and reported. By generating a controlled and reproducible artificial cough aerosol, the simulator allows us to conduct studies that cannot be carried out with human subjects.

The simulator produces a cough air flow comparable to that seen in human patients with respiratory infections (Figure 2). The bellows system is needed because the air brush by itself cannot generate enough air flow to match the cough profile and because varying the air pressure to the air brush to change the air flow would also change the particle size. The use of a linear motor allows coughs of different flow rates and volumes to be programmed into the control computer and permits fine-tuning the bellows movement to accurately reproduce coughs recorded from human subjects. The original simulator design used a piston-cylinder, but problems with friction from the seals and the need for wall lubrication led to a change to the bellows design. The bellows also acts as a spring, which provides a boost to the movement of the motor at the beginning of the cough when a rapid acceleration in air flow is needed. One disadvantage of the

bellows is that the many crevices make it more difficult to clean. We have found in practice that water-soluble aerosols rinse out reasonably well.

As noted in the Introduction, measurements of human cough aerosols have varied widely among researchers, with two fairly consistent features: the aerosol produced by coughing has a very broad size range, and the maximum number of particles almost always occurs in the smallest size bins. As can be seen in Figure 3, our simulator produces a cough aerosol containing particles with a lognormal size distribution from 0.1 to 100 µm when an air brush is used; 0.1 µm is the approximate size of a single influenza virion, while 100 µm is commonly used as the maximum size for aerosol particles. Alternatively, the nebulizer can be used to eliminate much of the larger fraction of the cough aerosol (Figure 6), which is useful when focusing on the role of smaller particles. A micropump nebulizer was used rather than a spray nebulizer because the micropump unit will aerosolize essentially all of the fluid added to it, it does not recirculate the fluid, and our tests indicated that the influenza virus used in our experiments survives aerosolization much better when using the micropump nebulizer rather than a spray nebulizer (data not shown).

The differences in the performance between the air brush and the nebulizer are clear in the volume-based distributions but are not as obvious in the count-based distributions because the number of small particles is much greater than the number of large ones, even though the collective volume of the smallest particles is relatively low. In addition, the fact that the highest numbers of particles are seen in the smallest size bins (especially for the nebulizer) suggests that the coughs may contain a substantial number of particles that are below the lower size limit of the aerosol measurement instrument (0.1 µm). If it were possible to measure these smallest particles, the differences in the count distributions of the cough aerosols from the air brush and the nebulizer might be more pronounced. In research on airborne disease transmission, the volume concentration of the aerosol particles is often more important than the count because the amount of pathogen is proportional to the total volume of the particles rather than

the number of particles (Nicas et al. 2005). However, count-based methods are widely used and are far more common in real-time instruments than are volume-based methods, and an understanding of both types of distributions and the limitations of attempts to convert from one to the other are critical when comparing results.

A few investigators have examined the mass or volume of particles ejected during a cough. The reported results have varied considerably with the different methods used and between subjects for each method. In an early study, Duguid (1946) collected coughed particles onto celluloid slides. He found that about 7.6 µl of droplets were expelled per cough, and that most of the volume was in larger particles; particles less than 100 µm in diameter only accounted for about 69 nl of the total. Zhu et al. (2006) had healthy subjects cough through surgical masks and then weighed the mask. They reported an average of 6.7 mg of droplets per cough for all particle sizes (no adjustment was made for evaporation). Xie et al. (2009) used a similar procedure and also had subjects cough into a bag. They measured an average of 1.1 mg of droplets per cough in each mask and 4.3 mg per cough in each bag. Lindsley et al. (2012) used an optical particle counter to estimate the dry volume of cough aerosol particles less than 10 µm in diameter from influenza patients. They found that each patient released 38 pl of particles in this size range per cough while sick and 26 pl per cough after recovery. At 68 µl, the aerosol output from the simulator is much greater than the actual aerosol output from a human cough. This is necessary in order to allow detection of the dispersed aerosol and viral particles, but may increase particle interactions in the aerosol.

The time course of the concentration of a cough aerosol during a human cough is unclear. One study indicated that the majority of the cough aerosol was contained in the initial part of a cough (Day et al. 2010), and this is consistent with theories about the sites of origin of aerosol particles in the respiratory tract (Johnson and Morawska 2009; Johnson et al. 2011). One initial idea for our cough simulator involved simply spraying the aerosol into the cough air as it was being coughed out. However, since the output from the air brush is constant while the air flow varies over the course of a cough, the

aerosol concentration would have been lowest during the highest flow period at the start of the cough, which is the opposite of what has been reported. Another possible method was to spray the aerosol into the cough bellows to load it with particles before coughing, but with this technique, large particles would tend to impact the walls or settle to the bottom before the cough and be lost. In addition, the aerosol concentration could be higher at the bottom of the bellows than at the top due to settling, especially for larger particles, which again could cause the concentration to be highest at the end of the cough. For these reasons, the PVC aerosol chamber was placed on top of the cough bellows as shown in Figure 1. The PVC chamber is long enough that the air brush can spray into it and create a cloud of particles with a broad size range, and it acts as a reservoir to give a higher concentration at the start of the cough. With this approach, the aerosol concentration is likely higher in the PVC chamber than it is in the bellows, and thus the aerosol concentration in the cough reaches an early peak during the cough and then falls to a lower level for both the air brush and the nebulizer (Figure 5 and Figure 8).

In the original cough simulator, a ball valve was used at the mouth to prevent aerosol particles from leaking from the simulator while loading it in preparation for a cough. The disadvantage of the ball valve is that it requires several seconds to open, allowing aerosol particles to settle inside the simulator before they can be coughed out. Solenoid valves are much faster but tend to collect aerosol particles because of the turns in the aerosol path. Instead, we added a vacuum scavenging port at the mouth of the simulator, which draws in air at 20 liters/second (about 2.4 times the output flow from the air brush). When the scavenger is activated, aerosol flowing toward the mouth of the simulator is drawn into the scavenger rather than leaving the mouth of the simulator, and outside air is drawn in through the mouth, preventing leakage prior to the cough. The scavenger is switched off just before the cough is initiated. An aerosol monitor outside the mouth of the simulator verified that no aerosol leakage occurred before coughing (data not shown).

In our experiments, we used a culture medium for propagating influenza virus since that is the focus of our work. Because solutions containing live influenza virus are biohazardous, decontamination of the simulator was an important consideration. The PVC chamber tends to accumulate liquid inside when used with the air brush. Thus, a gate valve was added to the lower part of the chamber to seal the bottom before removal. After detachment, the PVC chamber can be cleaned with a disinfectant solution in a biosafety cabinet. A similar PVC chamber is used with the micropump nebulizer, although no visible liquid accumulates inside because of the smaller particle-size output. The bellows-endplate assembly can be removed and autoclaved.

The cough aerosol simulator does have several limitations that need to be acknowledged. First, human cough aerosol measurements show a tremendous variation in quantity and size distribution. The output of the simulator is governed by the method of aerosol generation and the output parameters, and only represents two possible size distributions. Although the simulator output is similar to a human cough aerosol, it does not produce the full range of possible human cough aerosol outputs, and thus it may not be consistent with naturally-generated aerosols. Second, the cough produced by our simulator is not heated, while a human cough is typically warmer than the surrounding air and thus tends to be buoyant. This would not be expected to have a significant effect on large particles but likely would affect the behavior of smaller ones. Finally, the number of infectious agents per unit volume in the aerosol particles from the simulator is the same for all particle sizes. In human cough aerosols, this may not be the case because infecting microorganisms often are not uniformly distributed through the respiratory tract.

Conclusion

The cough aerosol simulator described here produces an aerosol with a broad size range and an air-flow profile similar to that of a human cough. The simulator can be used to study the distribution and fate of cough aerosols under controlled conditions and test the effect of different ventilation, disinfection, and personal protection methods. The

system can be used with live pathogens, which allows isolation precautions used in the healthcare field to be tested without risk of exposure for workers or patients. Future projects for the simulator include comparing the efficacy of different types of personal protective equipment, such as respirators, face shields, and powered air-purifying respirators. We also plan to test the effectiveness of placing loose-fitting face masks on patients as a method of reducing the release of infectious aerosols. The information gained from these tests will help us to better understand the transmission of infectious diseases, develop improved techniques for infection control and improve safety for healthcare workers and patients.

Acknowledgements

We would like to thank David Edgell of NIOSH for manufacturing many of the parts for the cough aerosol simulator. The findings and conclusions in this report are those of the authors and do not necessarily represent the views of the National Institute for Occupational Safety and Health.

Supplemental Information

A schematic of the measurement set-up, photographs and engineering drawings of the cough aerosol simulator are available online as supplemental information with this article at the journal's web site.

References

Brankston, G., Gitterman, L., Hirji, Z., Lemieux, C. , and Gardam, M. (2007). Transmission of influenza A in human beings, *Lancet Infect. Dis.* 7:257-65.

CDC. (2006). Interim guidance on planning for the use of surgical masks and respirators in health care settings during an influenza pandemic. Retrieved March 18, 2013, 2013, from http://home.nyc.gov/html/doh/downloads/pdf/bhpp/bhpp-interrim-maskguide120106.pdf.

Chao, C. Y. H., Wan, M. P., Morawska, L., Johnson, G. R., Ristovski, Z. D., Hargreaves, M., Mengersen, K., Corbett, S., Li, Y., Xie, X. , and Katoshevski, D. (2009). Characterization of

expiration air jets and droplet size distributions immediately at the mouth opening, *J. Aerosol Sci.* 40:122-133.

Day, J. B., Jones, B. M., Afshari, A. A., Frazer, D. G. , and Goldsmith, W. T. (2010). Temporal characteristics of aerosol generation during a voluntary cough [abstract]. *ATS 2010 International Conference*. New Orleans, LA USA, American Thoracic Society. 181: A2183.

Duguid, J. P. (1946). The size and the duration of air-carriage of respiratory droplets and droplet-nuclei, *J. Hyg. (Lond.)* 44:471-479.

Fabian, P., McDevitt, J. J., DeHaan, W. H., Fung, R. O., Cowling, B. J., Chan, K. H., Leung, G. M. , and Milton, D. K. (2008). Influenza virus in human exhaled breath: an observational study, *PLoS ONE* 3:e2691.

Fennelly, K. P., Jones-Lopez, E. C., Ayakaka, I., Kim, S., Menyha, H., Kirenga, B., Muchwa, C., Joloba, M., Dryden-Peterson, S., Reilly, N., Okwera, A., Elliott, A. M., Smith, P. G., Mugerwa, R. D., Eisenach, K. D. , and Ellner, J. J. (2012). Variability of infectious aerosols produced during coughing by patients with pulmonary tuberculosis, *Am. J. Respir. Crit. Care Med.* 186:450-7.

Goldmann, D. A. (2001). Epidemiology and prevention of pediatric viral respiratory infections in health-care institutions, *Emerg. Infect. Dis.* 7:249-53.

Gralton, J., Tovey, E., McLaws, M. L. , and Rawlinson, W. D. (2011). The role of particle size in aerosolised pathogen transmission: a review, *J. Infect.* 62:1-13.

Gupta, J. K., Lin, C. H. , and Chen, Q. (2009). Flow dynamics and characterization of a cough, *Indoor Air* 19:517-25.

Hall, C. B. (2007). The spread of influenza and other respiratory viruses: complexities and conjectures, *Clin. Infect. Dis.* 45:353-9.

Hui, D. S., Chow, B. K., Chu, L., Ng, S. S., Lee, N., Gin, T. , and Chan, M. T. (2012). Exhaled air dispersion during coughing with and without wearing a surgical or N95 mask, *PLoS ONE* 7:e50845.

Johnson, G. R. , and Morawska, L. (2009). The mechanism of breath aerosol formation, *J. Aerosol Med. Pulm. Drug Deliv.* 22:229-37.

Johnson, G. R., Morawska, L., Ristovski, Z. D., Hargreaves, M., Mengersen, K., Chao, C. Y. H., Wan, M. P., Li, Y., Xie, X., Katoshevski, D. , and Corbett, S. (2011). Modality of human expired aerosol size distributions, *J. Aerosol Sci.* 42:839-851.

Lindsley, W. G., Blachere, F. M., Thewlis, R. E., Vishnu, A., Davis, K. A., Cao, G., Palmer, J. E., Clark, K. E., Fisher, M. A., Khakoo, R. , and Beezhold, D. H. (2010). Measurements of airborne influenza virus in aerosol particles from human coughs, *PLoS ONE* 5:e15100.

Lindsley, W. G., King, W. P., Thewlis, R. E., Reynolds, J. S., Panday, K., Cao, G. , and Szalajda, J. V. (2012). Dispersion and exposure to a cough-generated aerosol in a simulated medical examination room, *J. Occup. Environ. Hyg.* 9:681-90.

Lindsley, W. G., Pearce, T. A., Hudnall, J. B., Davis, K. A., Davis, S. M., Fisher, M. A., Khakoo, R., Palmer, J. E., Clark, K. E., Celik, I., Coffey, C. C., Blachere, F. M. , and Beezhold, D. H. (2012). Quantity and size distribution of cough-generated aerosol particles produced by influenza patients during and after illness, *J. Occup. Environ. Hyg.* 9:443-9.

McCool, F. D. (2006). Global physiology and pathophysiology of cough: ACCP evidence-based clinical practice guidelines, *Chest* 129:48S-53S.

Monto, A. S. (2002). Epidemiology of viral respiratory infections, *Am. J. Med.* 112 Suppl 6A:4S-12S.

Morawska, L. (2006). Droplet fate in indoor environments, or can we prevent the spread of infection?, *Indoor Air* 16:335-47.

Morawska, L., Johnson, G. R., Ristovski, Z. D., Hargreaves, M., Mengersen, K., Corbett, S., Chao, C. Y. H., Li, Y. , and Katoshevski, D. (2009). Size distribution and sites of origin of droplets expelled from the human respiratory tract during expiratory activities, *J. Aerosol Sci.* 40:256-269.

Musher, D. M. (2003). How contagious are common respiratory tract infections?, *N. Engl. J. Med.* 348:1256-66.

Nicas, M., Nazaroff, W. W. , and Hubbard, A. (2005). Toward understanding the risk of secondary airborne infection: emission of respirable pathogens, *J. Occup. Environ. Hyg.* 2:143-54.

Noti, J. D., Blachere, F. M., McMillen, C. M., Lindsley, W. G., Kashon, M. L., Slaughter, D. R. , and Beezhold, D. H. (2013). High humidity leads to loss of infectious influenza virus from simulated coughs, *PLoS ONE* 8:e57485.

Noti, J. D., Lindsley, W. G., Blachere, F. M., Cao, G., Kashon, M. L., Thewlis, R. E., McMillen, C. M., King, W. P., Szalajda, J. V. , and Beezhold, D. H. (2012). Detection of infectious influenza virus in cough aerosols generated in a simulated patient examination room, *Clin. Infect. Dis.* 54:1569-77.

Pantelic, J., Sze-To, G. N., Tham, K. W., Chao, C. Y. H. , and Khoo, Y. C. M. (2009). Personalized ventilation as a control measure for airborne transmissible disease spread, *J. R. Soc. Interface* 6:S715-S726.

Roy, C. J. , and Milton, D. K. (2004). Airborne transmission of communicable infection--the elusive pathway, *New Eng. J. Med.* 350:1710-2.

Sattar, S. A. , and Ijaz, M. K. (2002). Airborne viruses. In *Manual of Environmental Microbiology*, edited by C. J. Hurst, R. L. Crawford, M. J. McInerney, G. R. Knudsen and L. D. Stetzenbach. ASM Press, Washington, DC, pp. 871-883.

Siegel, J. D., Rhinehart, E., Jackson, M. , and Chiarello, L. (2007). 2007 Guideline for isolation precautions: Preventing transmission of infectious agents in health care settings, *Am. J. Infect. Control* 35:S65-164.

Stelzer-Braid, S., Oliver, B. G., Blazey, A. J., Argent, E., Newsome, T. P., Rawlinson, W. D. , and Tovey, E. R. (2009). Exhalation of respiratory viruses by breathing, coughing, and talking, *J. Med. Virol.* 81:1674-9.

Tang, J. W., Liebner, T. J., Craven, B. A. , and Settles, G. S. (2009). A schlieren optical study of the human cough with and without wearing masks for aerosol infection control, *J. R. Soc. Interface* 6:S727-S736.

Tang, J. W., Nicolle, A. D., Pantelic, J., Jiang, M., Sekhr, C., Cheong, D. K. , and Tham, K. W. (2011). Qualitative real-time schlieren and shadowgraph imaging of human exhaled airflows: an aid to aerosol infection control, *PLoS ONE* 6:e21392.

Tellier, R. (2009). Aerosol transmission of influenza A virus: a review of new studies, *J. R. Soc. Interface* 6 Suppl 6:S783-90.

To, G. N. S., Wan, M. P., Chao, C. Y. H., Fang, L. , and Melikov, A. (2009). Experimental study of dispersion and deposition of expiratory aerosols in aircraft cabins and impact on infectious disease transmission, *Aerosol Sci. Technol.* 43:466-485.

VanSciver, M., Miller, S. , and Hertzberg, J. (2011). Particle image velocimetry of human cough, *Aerosol Sci. Technol.* 45:415-422.

Wan, M. P., Chao, C. Y. H., Ng, Y. D., Sze To, G. N. , and Yu, W. C. (2007). Dispersion of expiratory droplets in a general hospital ward with ceiling mixing type mechanical ventilation system, *Aerosol Sci. Technol.* 41:244-258.

Weber, T. P. , and Stilianakis, N. I. (2008). Inactivation of influenza A viruses in the environment and modes of transmission: a critical review, *J. Infect.* 57:361-73.

Xie, X., Li, Y., Sun, H. , and Liu, L. (2009). Exhaled droplets due to talking and coughing, *J. R. Soc. Interface* 6 Suppl 6:S703-14.

Zhu, S. W., Kato, S. , and Yang, J. H. (2006). Study on transport characteristics of saliva droplets produced by coughing in a calm indoor environment, *Build. Environ.* 41:1691-1702.

Figures

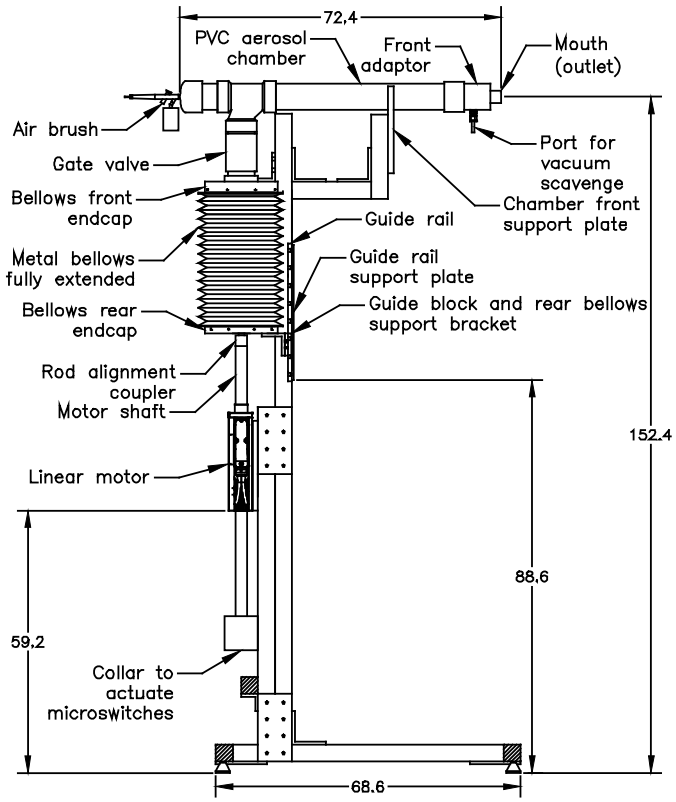

Figure 1: Schematic of the cough aerosol simulator with air brush. Dimensions are in centimeters. The air brush generates the test aerosol by spraying media into the PVC chamber. The aerosol is also drawn into the bellows as the bellows is pulled down in preparation for a cough. When a cough is triggered, the linear motor pushes the bellows upward, driving the aerosol out of the mouth of the simulator and producing the cough.

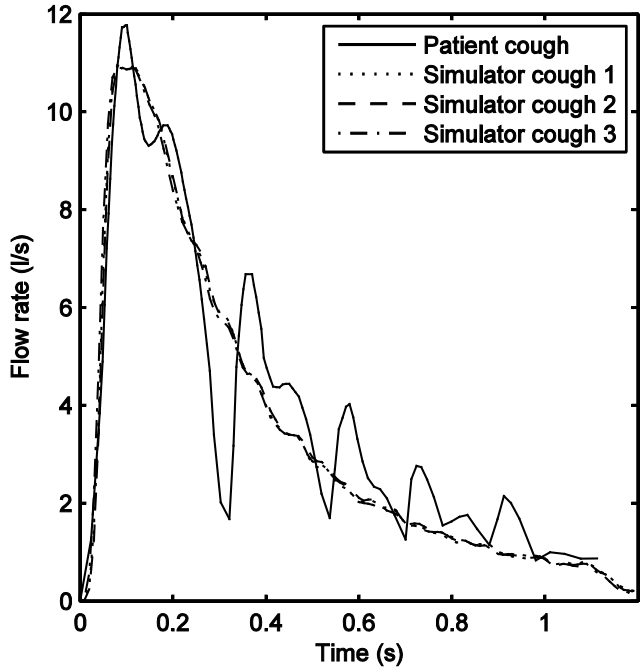

Figure 2: Cough flow rate vs. time for influenza patient and cough simulator. The correlation coefficients between the patient cough and the three simulator coughs were 0.92, 0.92, and 0.91.

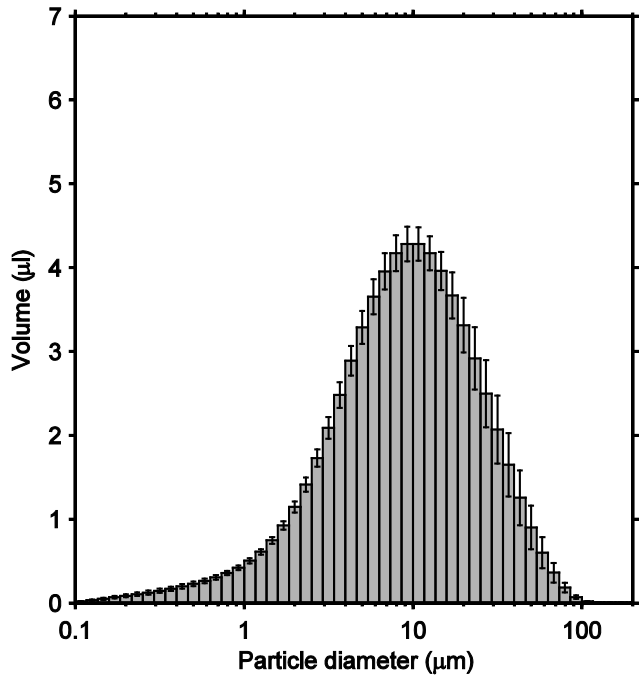

Figure 3: Volume-based size distribution of the simulated cough aerosol using the air brush. The distribution is for all particles expelled over the course of a cough. It has a VMD of 8.46 µm and a GSD of 2.86. The plot shows the mean of 10 experiments. Error bars show the standard deviation.

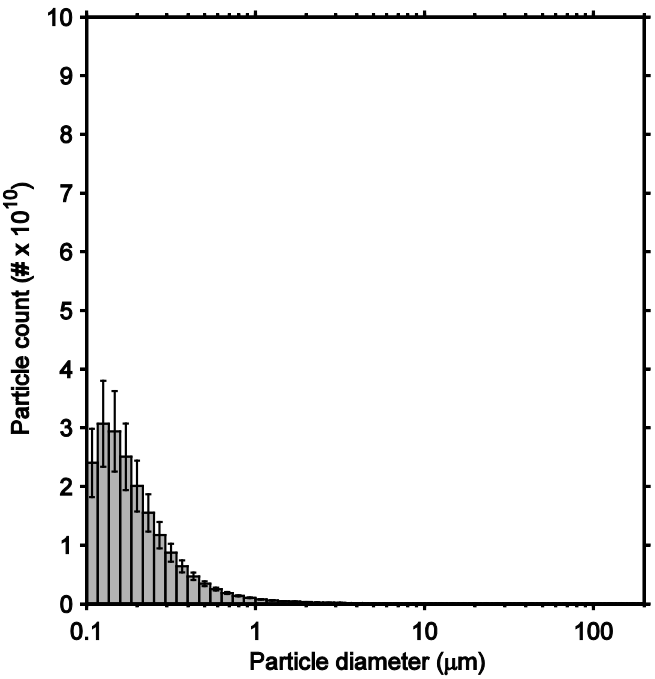

Figure 4: Count-based size distribution of the simulated cough aerosol using the air brush. The distribution is for all particles expelled over the course of a cough. It has a CMD of 0.194 µm and a GSD of 1.73. The plot shows the mean of 10 experiments. Error bars show the standard deviation.

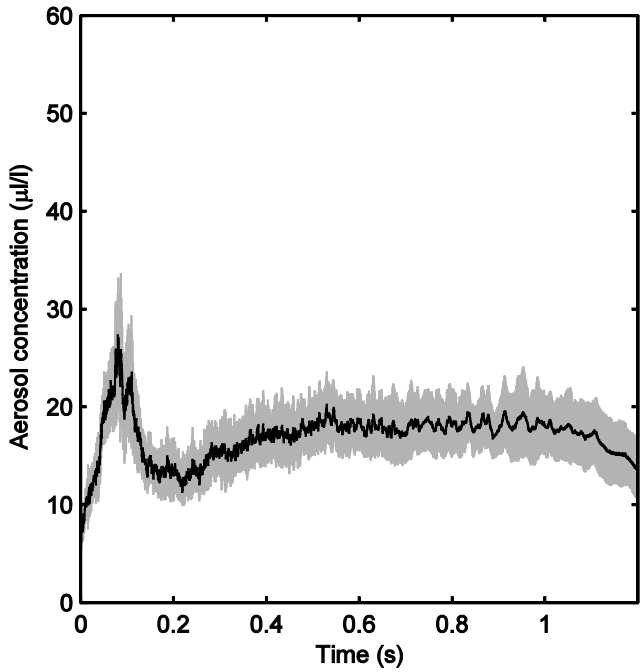

Figure 5: Aerosol concentration over time during a cough using the air brush. The black line is the mean of 10 experiments. The shaded region is ±1 standard deviation.

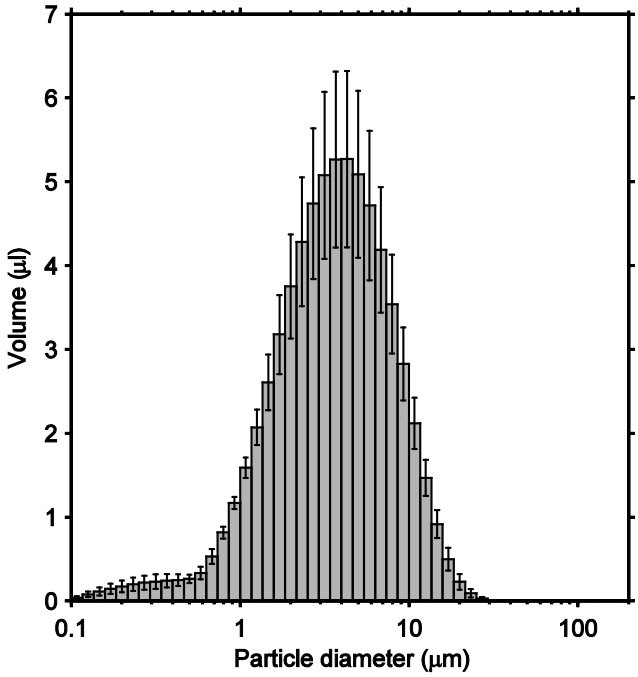

Figure 6: Volume-based size distribution of the simulated cough aerosol using the Aeroneb nebulizer. The distribution is for all particles expelled over the course of a cough. It has a VMD of 3.39 µm and a GSD of 2.32. The plot shows the mean of 8 experiments. Error bars show the standard deviation.

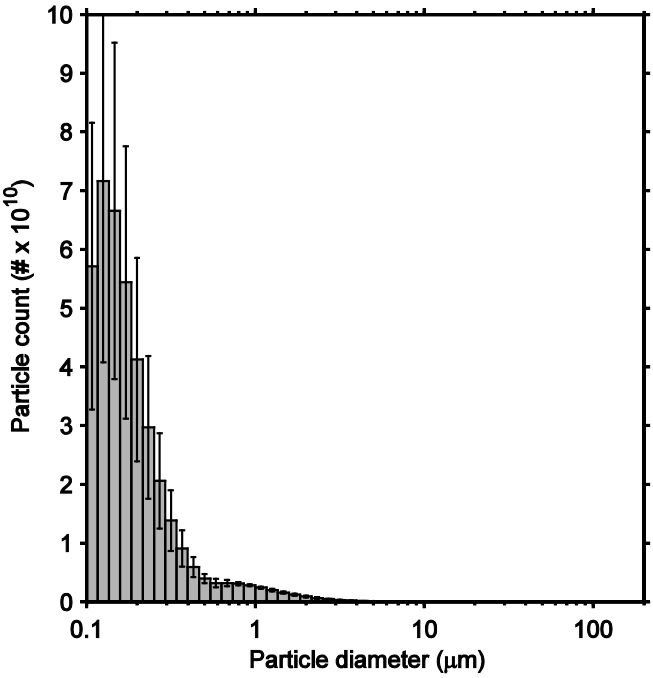

Figure 7: Count-based size distribution of the simulated cough aerosol using the nebulizer. The plot shows the mean of 8 experiments. The distribution has a CMD of 0.185 µm and a GSD of 1.75. Error bars show the standard deviation.

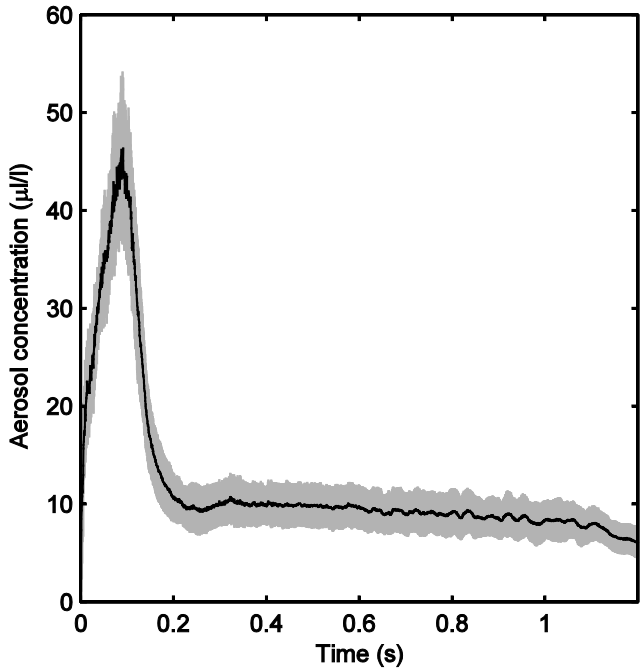

Figure 8: Aerosol concentration over time during a cough using the nebulizer. The black line is the mean of 8 experiments. The shaded region is ±1 standard deviation.

Supplemental information

A Cough Aerosol Simulator for the Study of Disease Transmission by Human Cough-Generated Aerosols

William G. Lindsley, Jeffrey S. Reynolds, Jonathan V. Szalajda, John D. Noti, and Donald H. Beezhold

Schematic of the cough aerosol measurement set-up

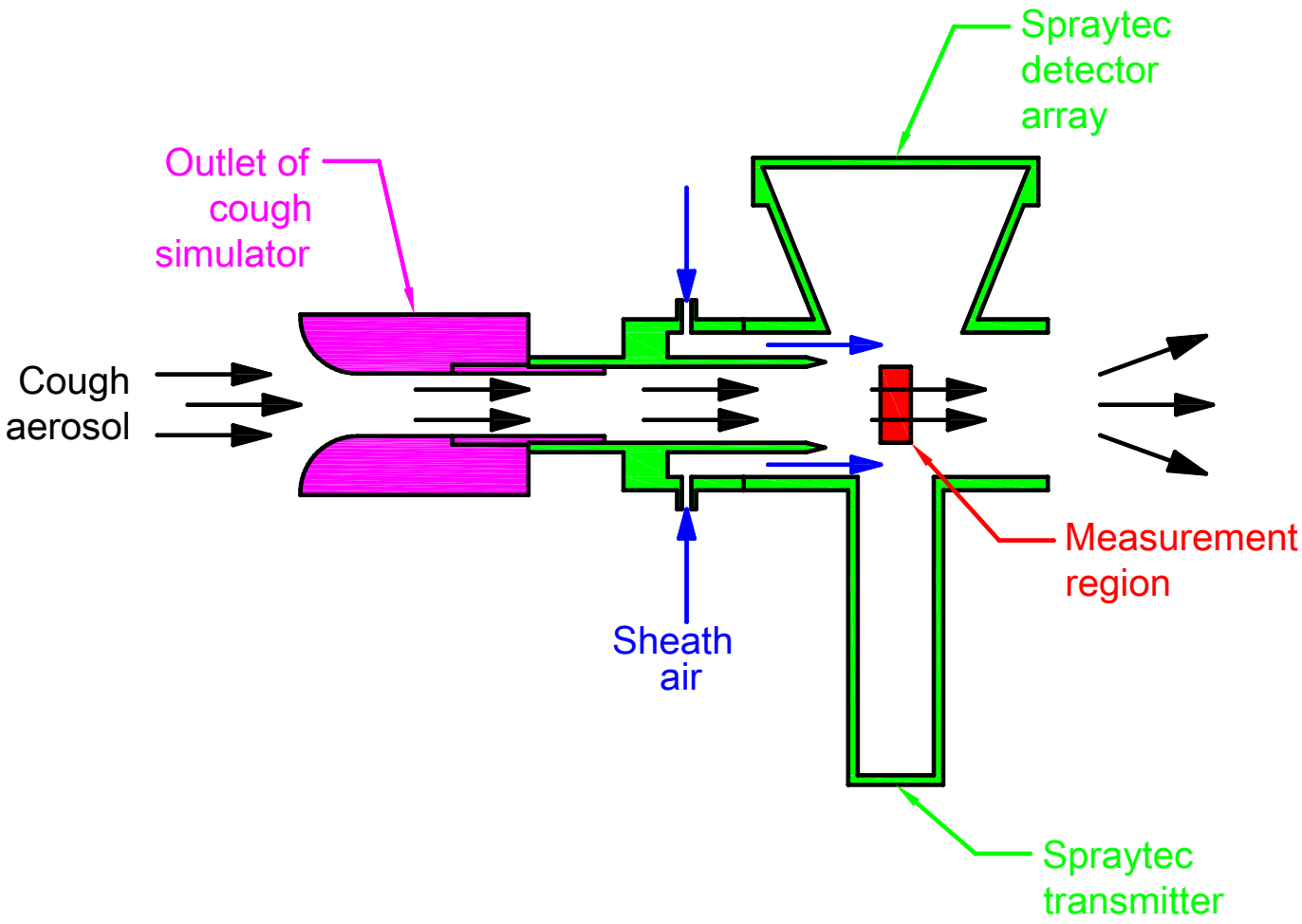

This schematic shows a top cross-sectional view of the aerosol measurement system. A Spraytec "inhalation cell" was used with the spray measurement system so that the aerosol was kept separated from the environment before measurement. The inhalation cell (green) was attached to the outlet of the cough simulator (magenta). The cough aerosol (black arrows)

flowed out of the simulator and into the measurement region of the Spraytec (red). The measurement region has a cylindrical shape 25.4 mm long and 10 mm in diameter. At the end of the cough, the simulator bellows was held in the compressed position until the measurement was completed so that outside aerosol particles would not be drawn back into the instrument. Six liters/minute of sheath air (blue) was used to help keep the aerosol from entering the transmitter and detector regions and to prevent recirculation.

Photos of the cough simulator

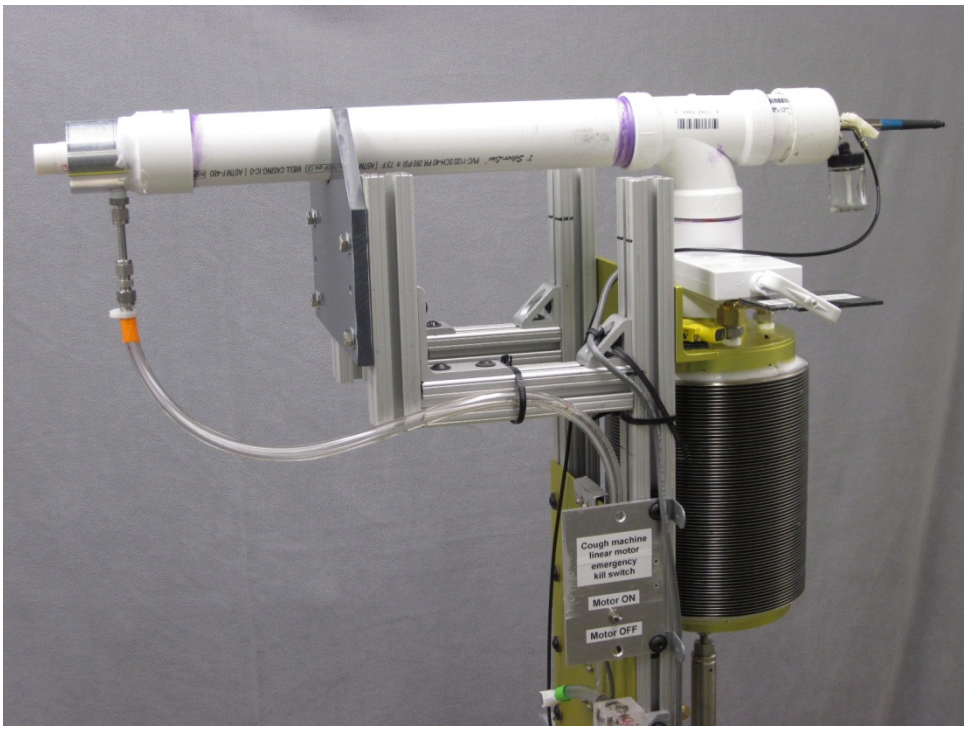

Top of the cough aerosol simulator. The white tube is the PVC aerosol chamber. The air brush, which can be seen at the right end of the PVC chamber, sprays into the chamber to load the simulator with aerosol particles. The glass jar attached to the bottom of the air brush contains the spray fluid. The cough exits horizontally out of the small PVC tube on the left.

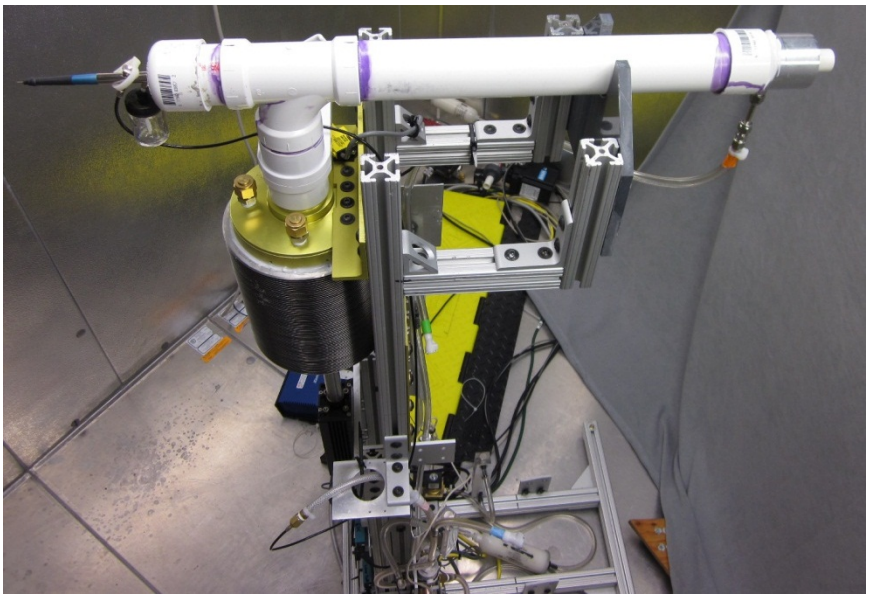

Another view of the top of the simulator showing the support frame supporting the aerosol chamber. The support frame of the simulator was assembled from T-slot structural aluminum (80/20, Inc.).

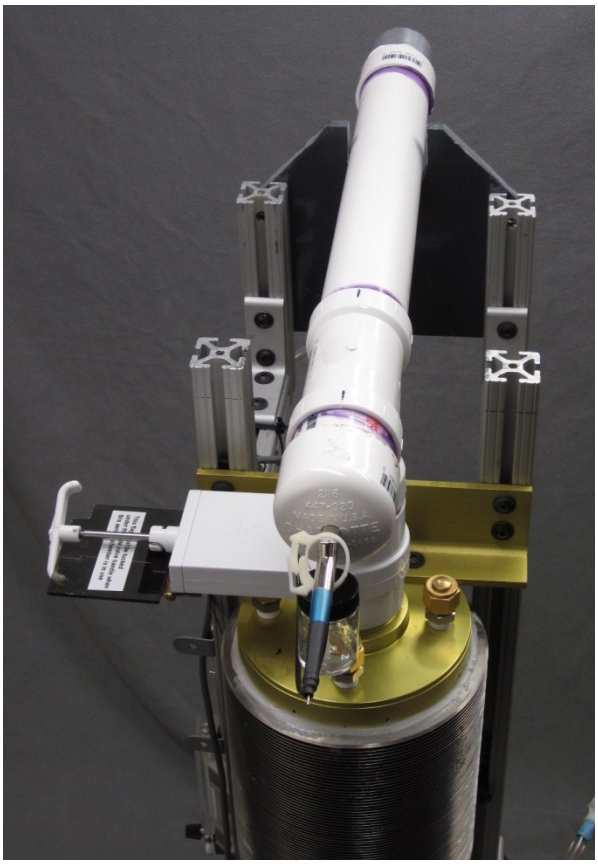

The air brush can be seen at the rear of the PVC chamber. The white handle on the left opens and closes the gate valve at the bottom

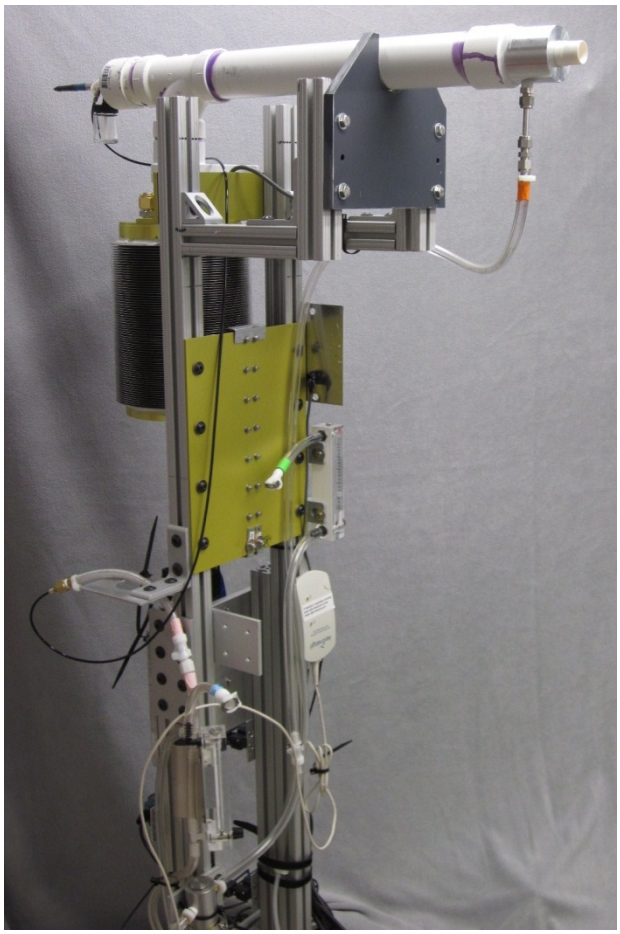

Front quarter view of the simulator. The tube extending from the bottom of the aluminum adaptor in the front section of the PVC

of the PVC chamber.

chamber is the vacuum scavenger line. It leads to a vacuum trap and then to a house vacuum line.

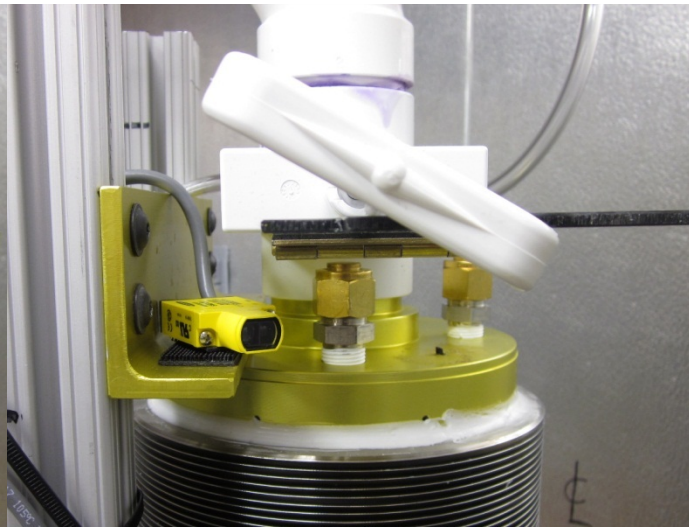

To ensure that the gate is open before coughing, a plastic hinged flap is attached beneath the valve. An infrared sensor (the small yellow box with the black lens on front) detects the flap when it is down as seen here and prevents the simulator from coughing.

When the gate valve is fully opened, the plastic flap can be tucked beneath the handle as shown. The flap then is not detected by the infrared sensor, and the control program will permit a cough to be triggered.

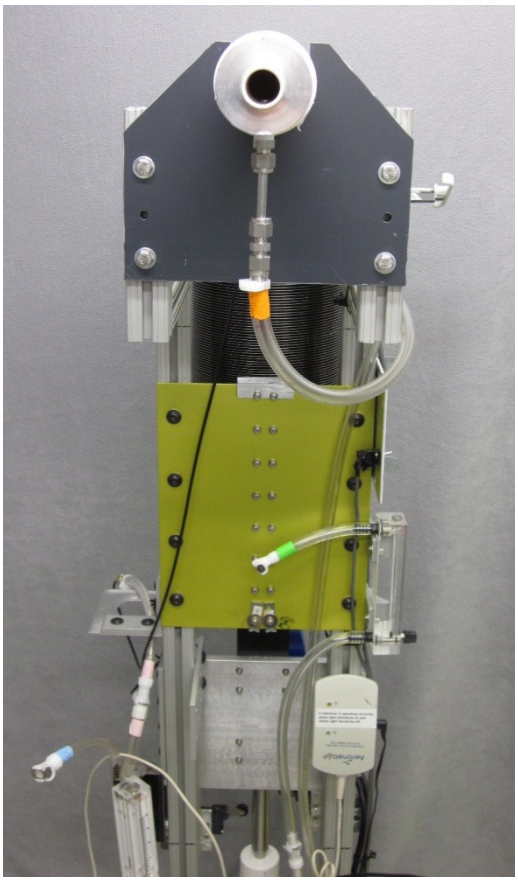

Front view of the simulator showing the vacuum scavenger line, the grey front support plate and the yellow bellows guide rail support plate. The white box at the lower right is the power supply for the Aeroneb micropump nebulizer.

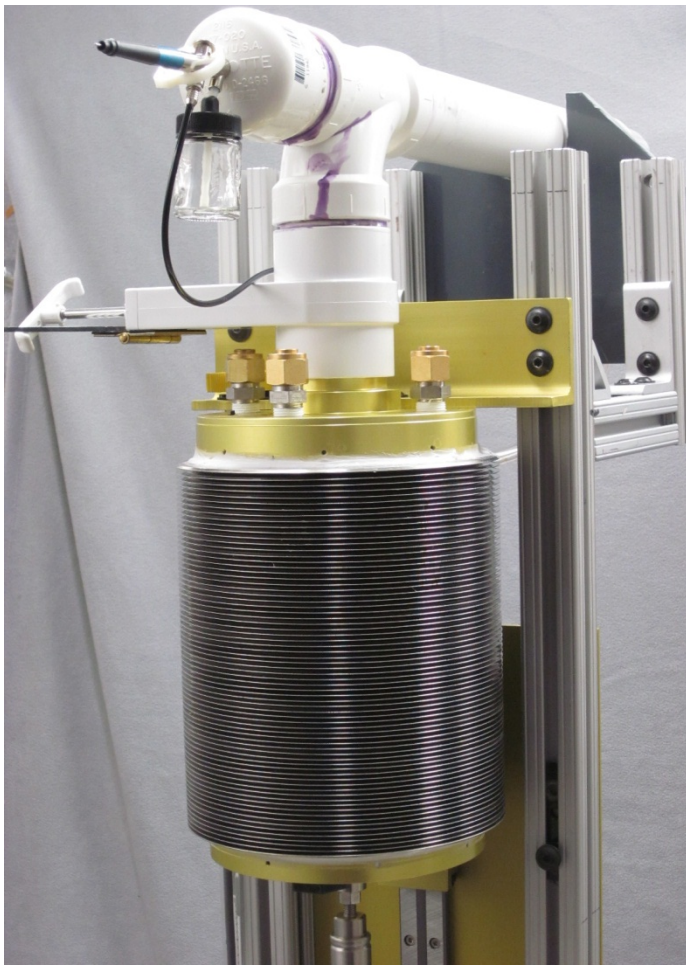

Rear quarter view of the simulator showing the stainless steel bellows. The yellow front end cap for the bellows (on top of the bellows in this picture) has three ports with brass caps that can be used for instrumentation, sampling probes and cleaning. The bellows assembly has two custom-made aluminum end caps which were anodized to resist corrosion. The bellows is held to the end caps by a ring of cone-point set screws and sealed with silicone sealant. The upper end cap of the bellows assembly is fixed in place by a bracket fastened to the support frame. The lower end cap is attached to a slide and rail to support and steady it during movement. The lower end cap is

also attached to the linear motor shaft by a rod alignment coupler, which allows the motor to move the end cap up and down, compressing and expanding the bellows.

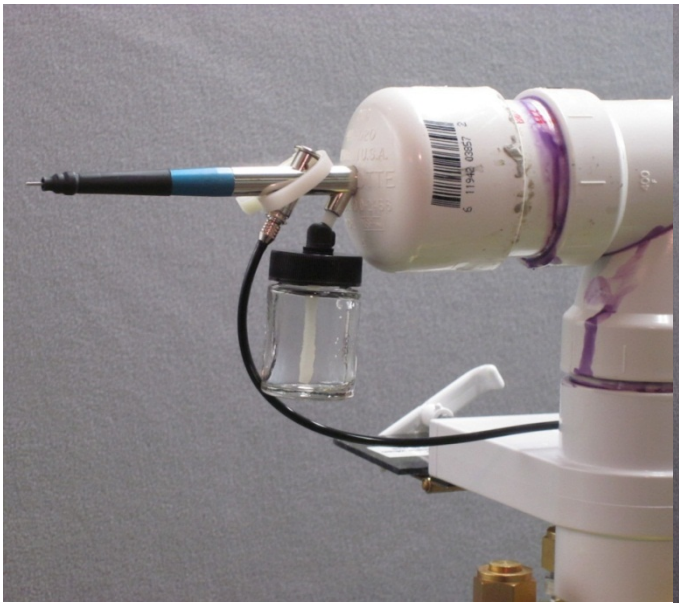

Close view of the air brush attached to the back of the PVC aerosol chamber. A hole bored in the end cap provides a tight fit around the air brush barrel, which is held in place by friction.

Shown here is a different version of the PVC chamber used with the Aeroneb nebulizer to produce a smaller aerosol.

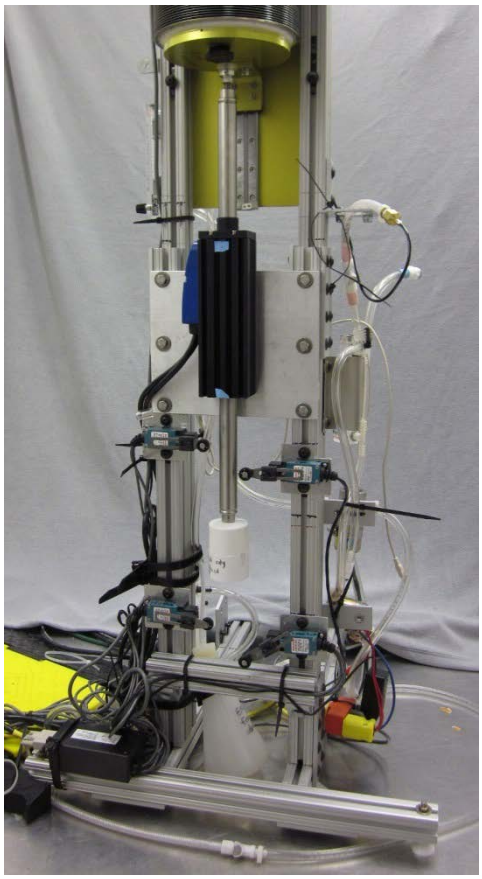

The Copley linear motor (black rectangular box in the center of the picture) provides the thrust to compress and expand the bellows.

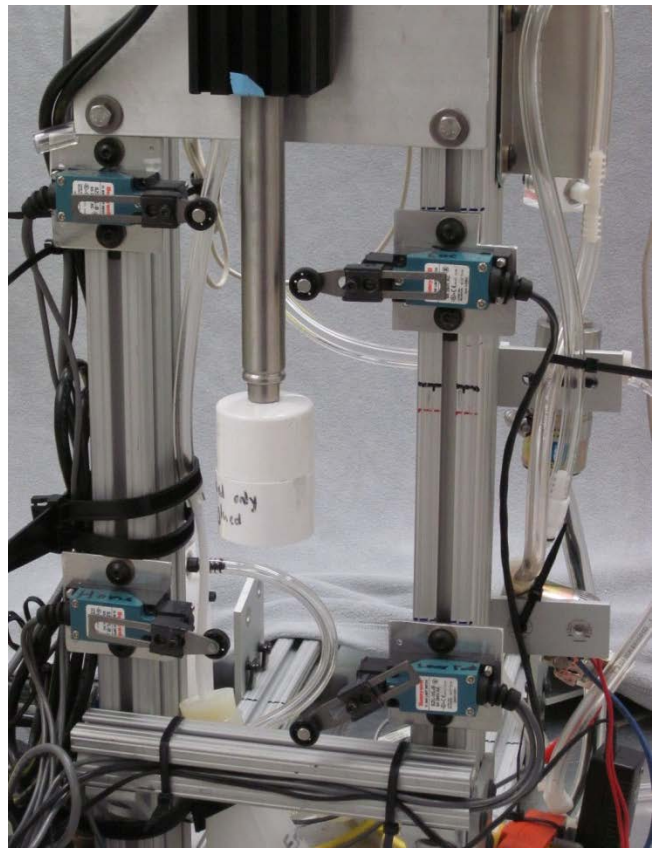

Four microswitches (light blue rectangular boxes with black wheels on arms) signal the position of the motor shaft. The top and bottom switches stop the motor if it travels too far up or down. The second-lowest switch (on the left) indicates when the shaft has reached the home reference position. The second-highest switch (on the right) indicates when the shaft has reached the end of a cough. The white PVC cylinder in the center actuates the switches.

Simulator control software

The control software for the simulator was written using LabVIEW, which is available commercially from National Instruments (http://www.ni.com). Copley Motion (http://www.copleymotion.com) supplies LabVIEW drivers for their linear motor which were incorporated into the control program. The control program is available upon request from the corresponding author (Dr. William G. Lindsley, wlindsley@cdc.gov), but does require LabVIEW to run.

Engineering drawings included in the supplemental information

Engineering drawings of the different parts of the cough simulator are shown below. All dimensions are in inches except as noted. All drawings are available upon request from the corresponding author (Dr. William G. Lindsley, wlindsley@cdc.gov) in DWG format, which is the standard format for AutoCAD and can be read by many other drafting programs. Autodesk also offers a free DWG drawing viewer program at http://usa.autodesk.com.

Drawing name	*Description*
Annotated overall drawing of cough simulator	Overall schematic of the cough aerosol simulator showing the major parts.
Cough simulator support frame	Dimensions and layout of the simulator support frame with brackets and mounting plates.
Assembly detail for motor & bellows	Detailed schematic of the linear motor, metal bellows, end caps and attachment brackets and plates.
Air brush PVC chamber	Dimensions and layout of the PVC aerosol chamber used with the air brush.
Aeroneb PVC chamber	Dimensions and layout of the PVC aerosol chamber used with the Aeroneb nebulizer.
2 in cough simulator adaptor	Aluminum adaptor at the front of the PVC aerosol chamber. The simulator mouthpiece and the vacuum scavenger attach to this adaptor.
Bellows back bracket	Bracket attaching the rear bellows end plate to the guide block on the guide rail.
Bellows front bracket	Bracket attaching the front bellows end plate to the support frame.
Bellows guide rail support plate	Plate attached to the support frame that holds the guide rail.
Cough sim bellows back	Rear end plate that attaches to the metal bellows and to the guide block.
Cough sim bellows front	Front end plate that attaches to the metal bellows and the support frame.

Linear motor mounting plate	Support plate that attaches the linear motor to the support frame.
PVC chamber front support plate	PVC plate that supports the front part of the PVC aerosol chamber.

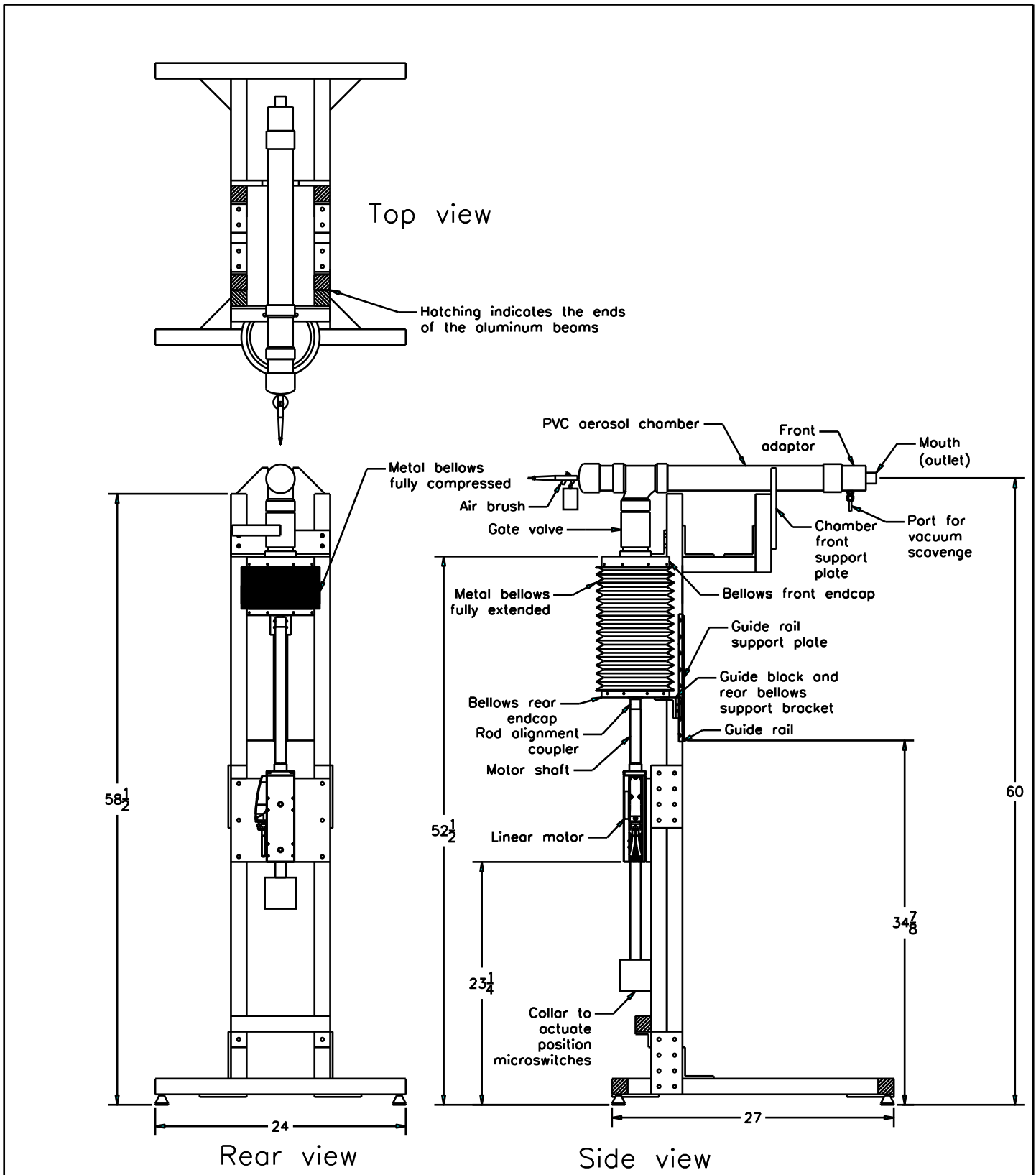

Unless otherwise specified: Dimensions are in inches Break all edges 0.01 max Remove all burrs Tolerances are: .XX ±.01 .XXX ±.005 Angles 0.5° Fractional ±1/32	Cough simulator
	Date: 2/21/2013
	Drawn by: William G. Lindsley
Annotated overall drawing of cough simulator.dwg	Scale: Sheet 1 of 1

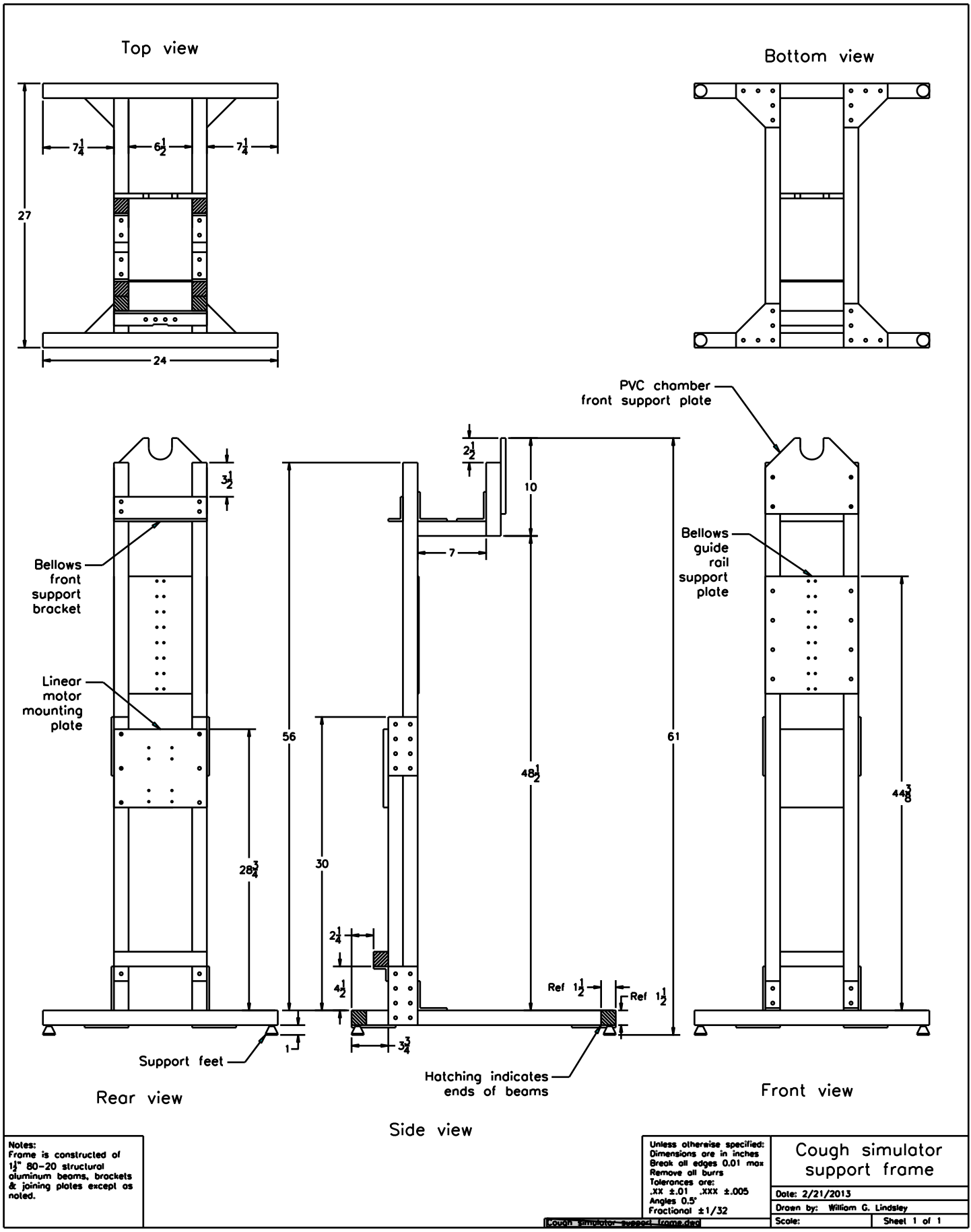

Notes:
Frame is constructed of 1½" 80-20 structural aluminum beams, brackets & joining plates except as noted.

Unless otherwise specified:
Dimensions are in inches
Break all edges 0.01 max
Remove all burrs
Tolerances are:
.XX ±.01 .XXX ±.005
Angles 0.5°
Fractional ±1/32

Cough simulator support frame.dwg

Cough simulator support frame

Date: 2/21/2013
Drawn by: William G. Lindsley
Scale:
Sheet 1 of 1

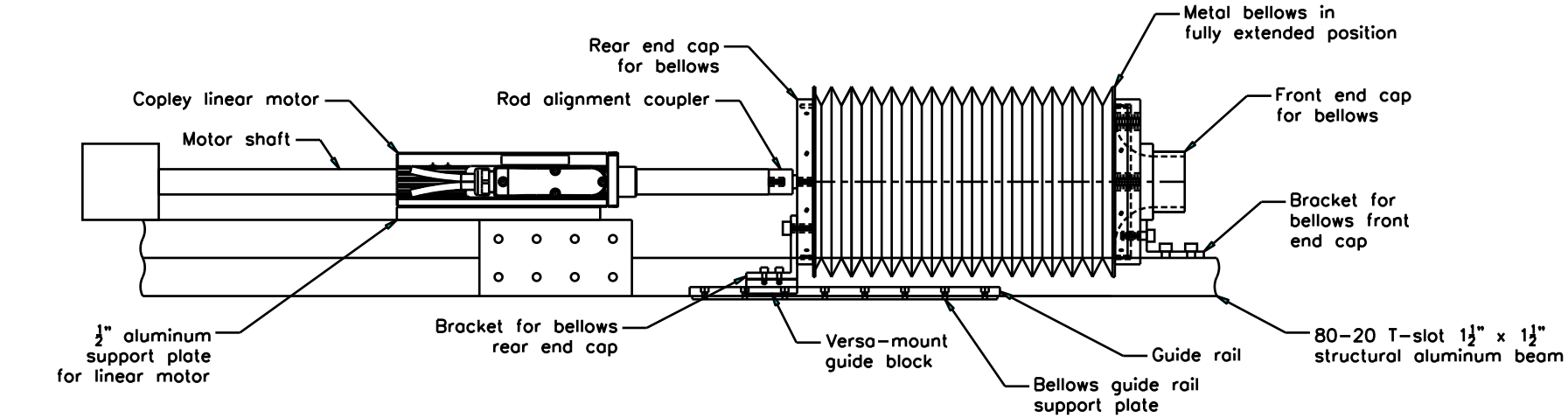

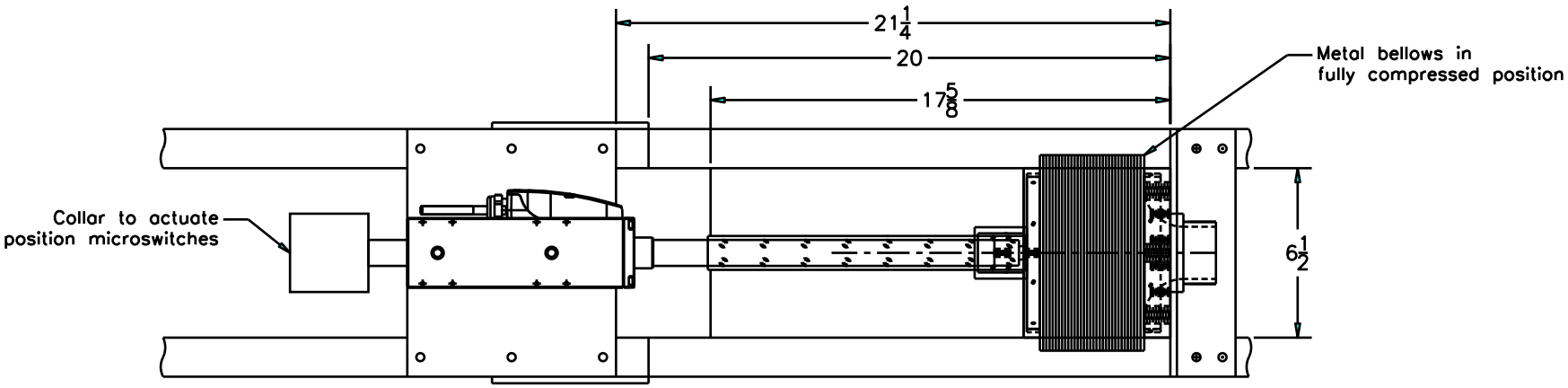

Unless otherwise specified:
Dimensions are in inches
Break all edges 0.01 max
Remove all burrs
Tolerances are:
.XX ±.01 .XXX ±.005
Angles 0.5°
Fractional ±1/32

Assembly detail for motor & bellows.dwg

Bellows cough simulator assembly

Date: 2/20/2013

Drawn by: William G. Lindsley

Scale: 1/4

Sheet 1 of 1

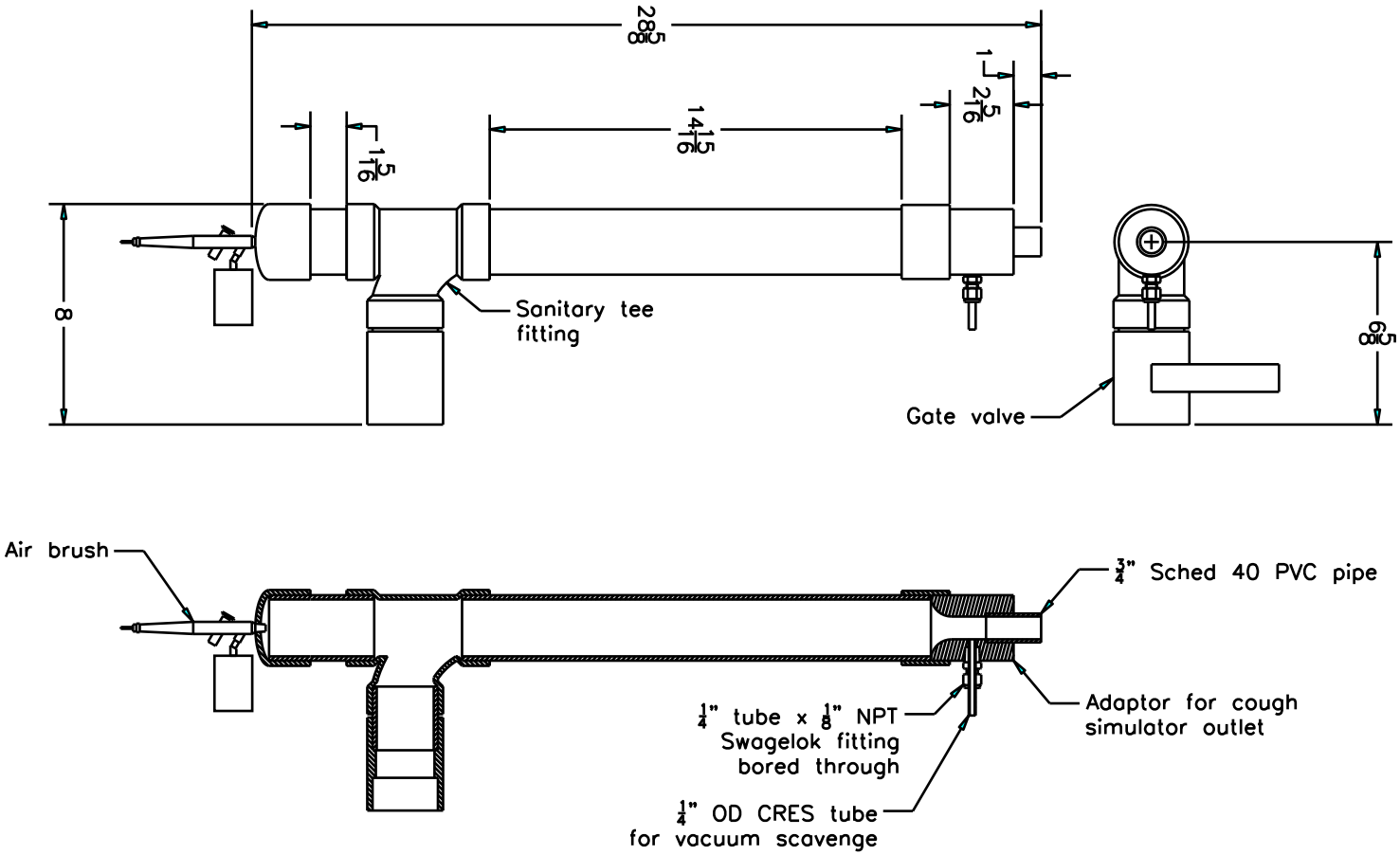

Notes:
1. All pipe and fittings are 2" Schedule 40 PVC except as noted.

Unless otherwise specified:
Dimensions are in inches
Break all edges 0.01 max
Remove all burrs
Tolerances are:
.XX ±.01 .XXX ±.005
Angles 0.5°
Fractional ±1/32

Air brush PVC chamber.dwg

PVC cough aerosol chamber

Date: 2/13/2013

Drawn by: William G. Lindsley

Scale: 1/4

Sheet 1 of 1

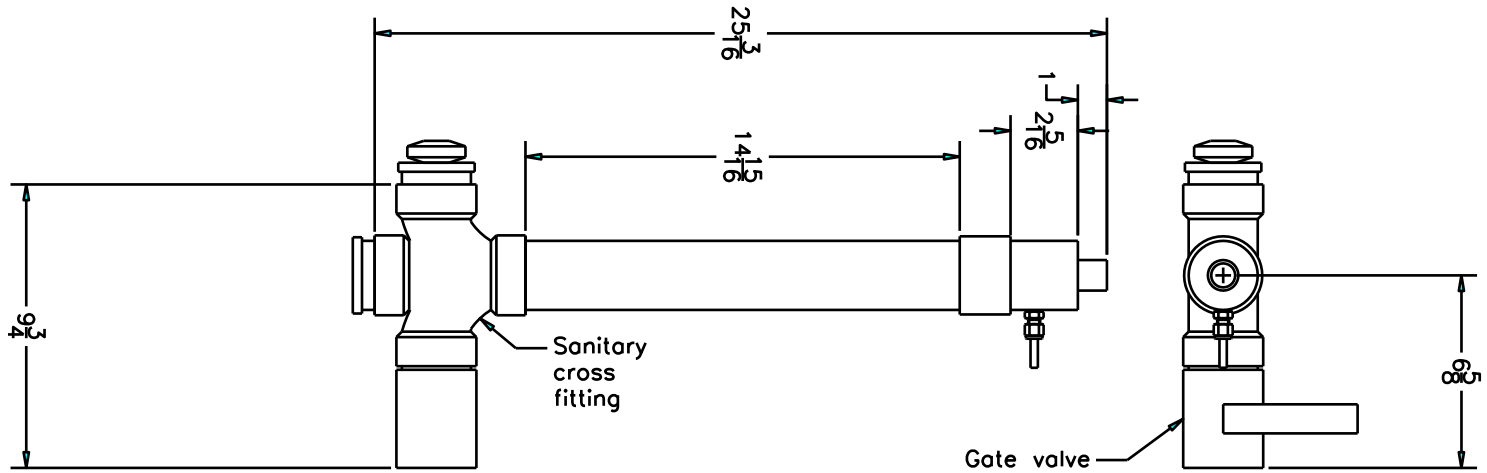

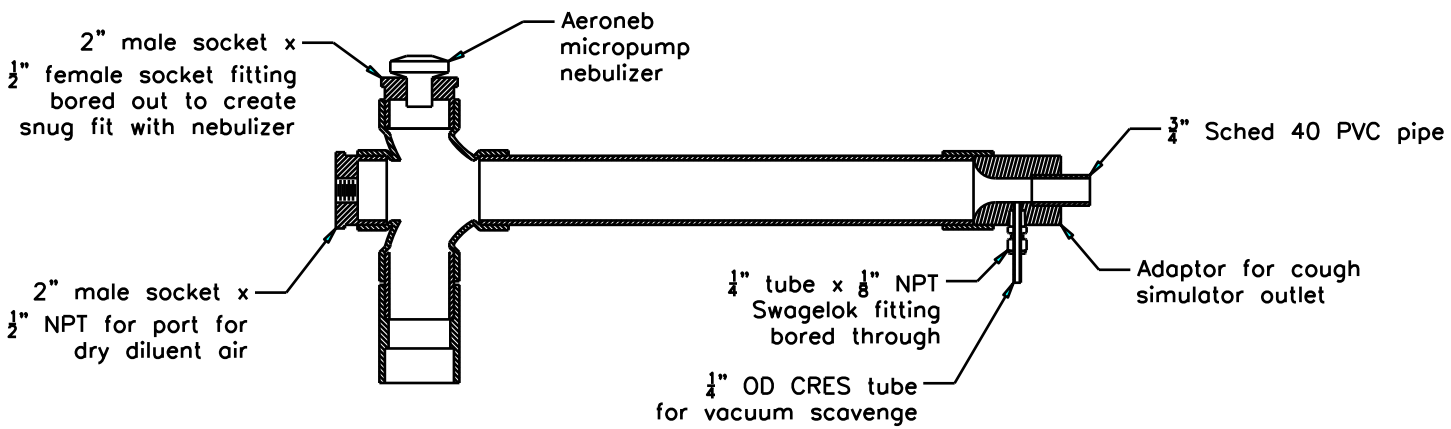

Notes:
1. All pipe and fittings are 2" Schedule 40 PVC except as noted.

Unless otherwise specified:
Dimensions are in inches
Break all edges 0.01 max
Remove all burrs
Tolerances are:
.XX ±.01 .XXX ±.005
Angles 0.5°
Fractional ±1/32

Aeroneb PVC chamber.dwg

Nebulizer PVC cough aerosol chamber

Date: 2/13/2013

Drawn by: William Lindsley

Scale: 1/4

Sheet 1 of 1

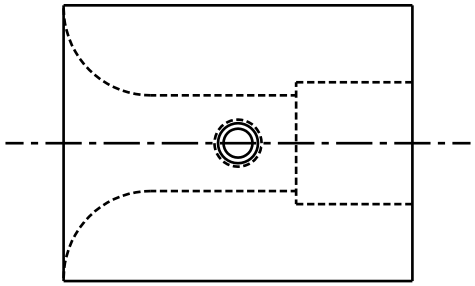

Section AA

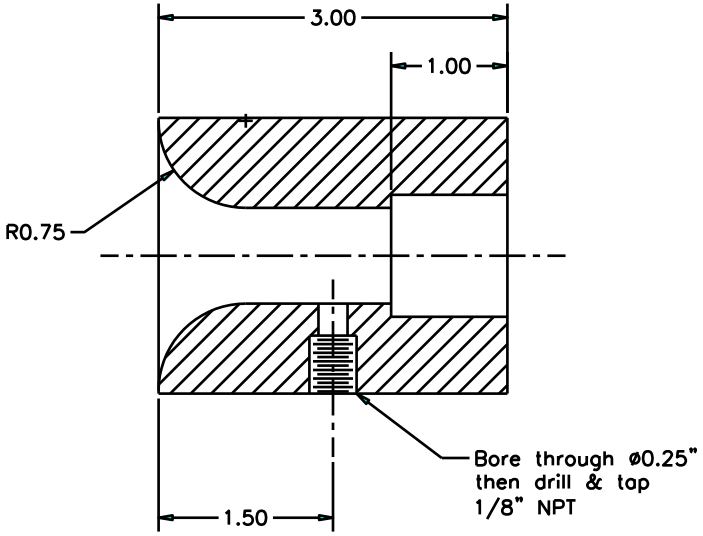

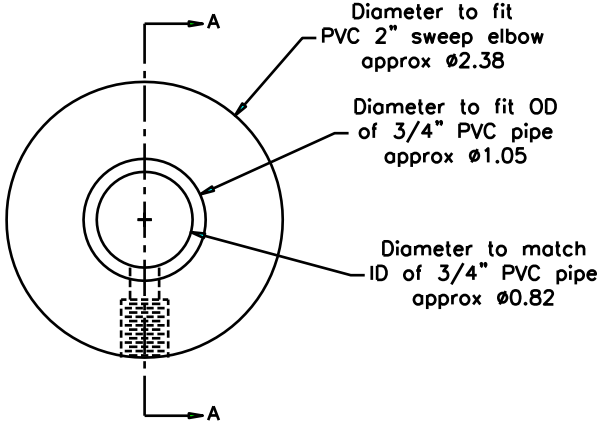

Notes:
1. Adaptor to fit 2" PVC coupling.
2. Material 6061 Al
3. Finish Anodize
4. One required

Unless otherwise specified:
Dimensions are in inches
Break all edges 0.01 max
Remove all burrs
Tolerances are:
.XX ±.01 .XXX ±.005
Angles 0.5°
Fractional ±1/32

2 in cough simulator adaptor.dwg

Adaptor for cough simulator outlet

Date: 2/13/2013

Drawn by: William G. Lindsley

Scale: 1/1

Sheet 1 of 1

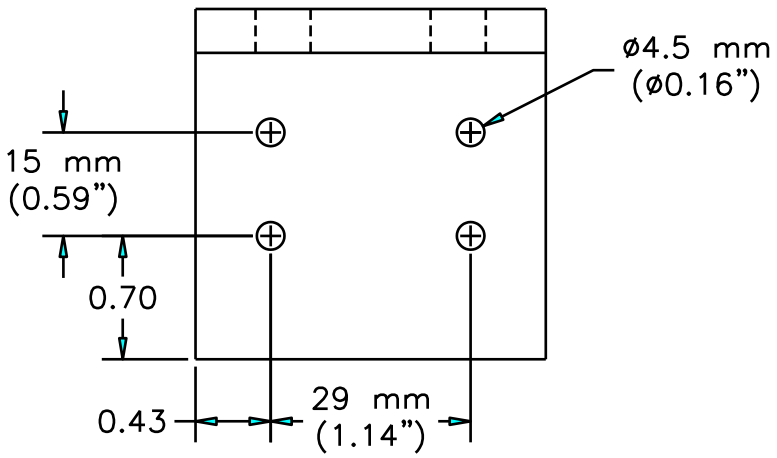

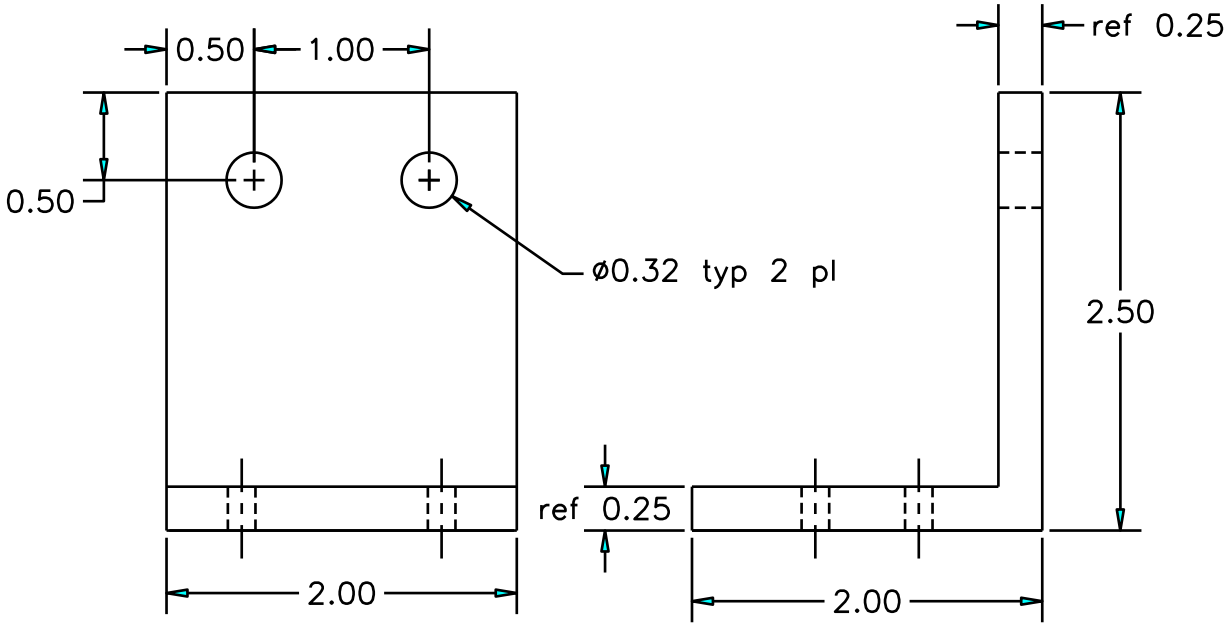

Notes:
1. Material 6061 Al
2. Finish anodize.
3. One required

Unless otherwise specified:
Dimensions are in inches
Break all edges 0.01 max
Remove all burrs
Tolerances are:
.XX ±.01 .XXX ±.005
Angles 0.5°
Fractional ±1/32

Bellows back bracket.dwg

Bracket for bellows rear end cap

Date: 2/22/2013

Drawn by: William G. Lindsley

Scale: 1/1

Sheet 1 of 1

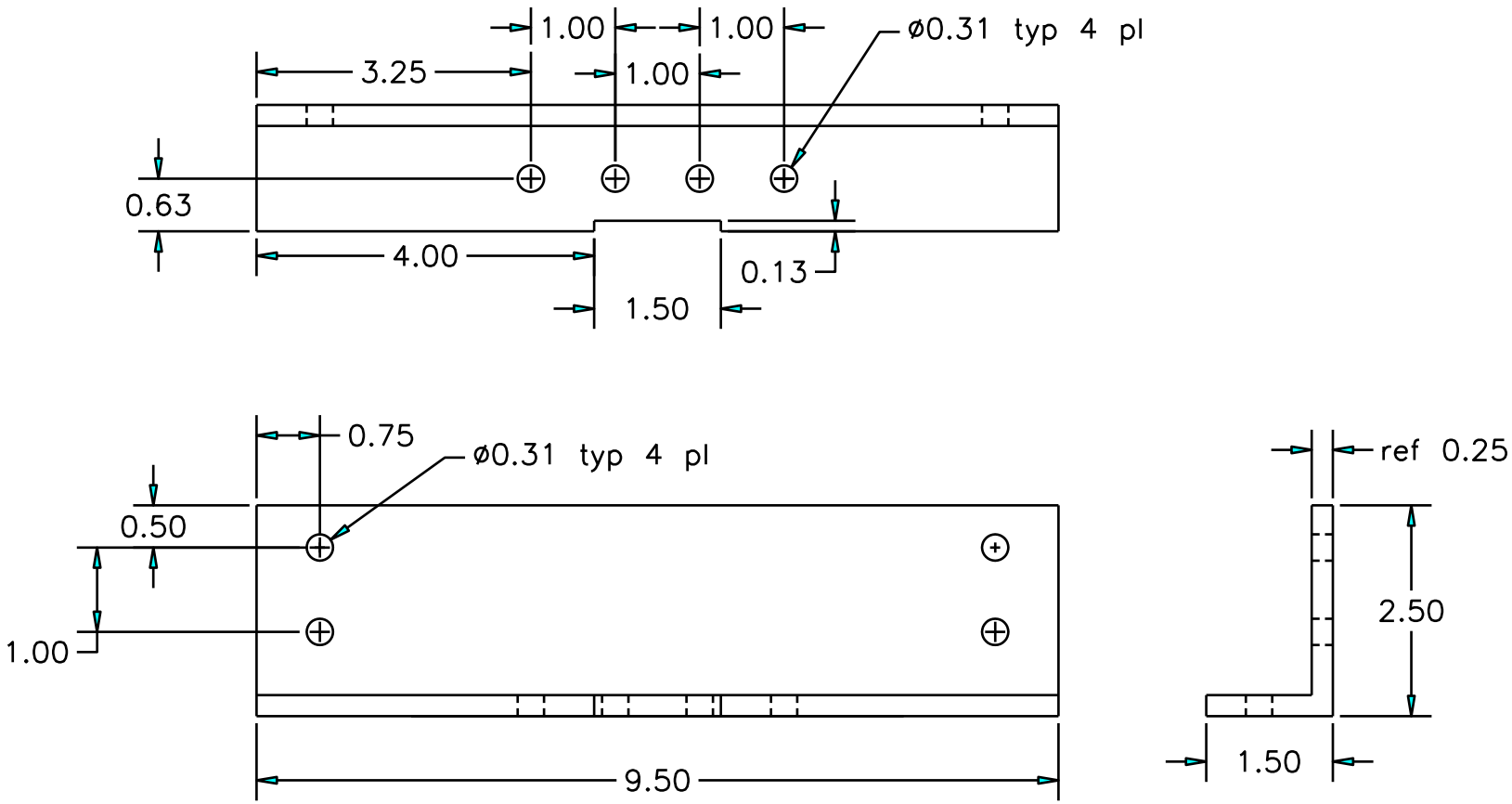

Notes
1. Material 6061 Al
2. Finish anodize.
3. One required

Bellows front bracket.dwg

Unless otherwise specified:
Dimensions are in inches
Break all edges 0.01 max
Remove all burrs
Tolerances are:
.XX ±.01 .XXX ±.005
Fraction 1/32 Angles 0.5°

Bellows front support bracket

Date: 2/21/2013

Drawn by: William G. Lindsley

Scale: 1/2

Sheet 1 of 1

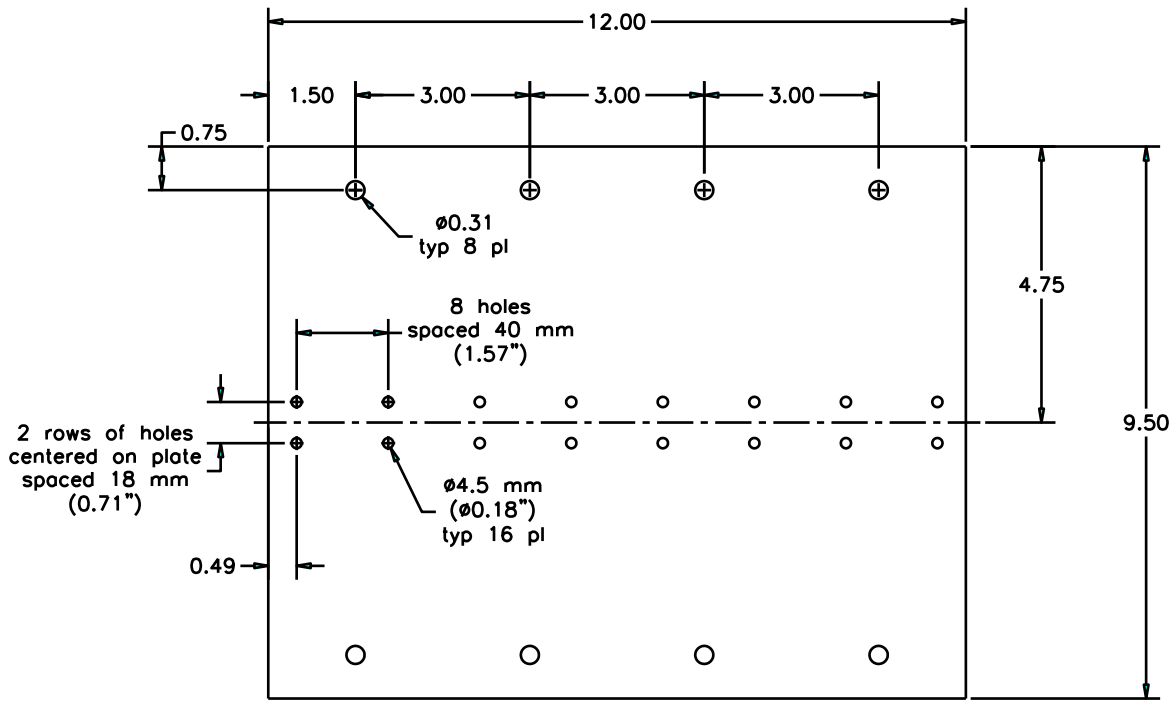

Notes:
1. Material 1/8" thick 6061 Al plate
2. Finish anodize.
3. One required.

Unless otherwise specified:
Dimensions are in inches
Break all edges 0.01 max
Remove all burrs
Tolerances are:
.XX ±.01 .XXX ±.005
Angles 0.5°
Fractional ±1/32

Bellows guide rail support plate.dwg

Bellows guide rail support plate

Date: 2/21/2013

Drawn by: William G. Lindsley

Scale: 1/2

Sheet 1 of 1

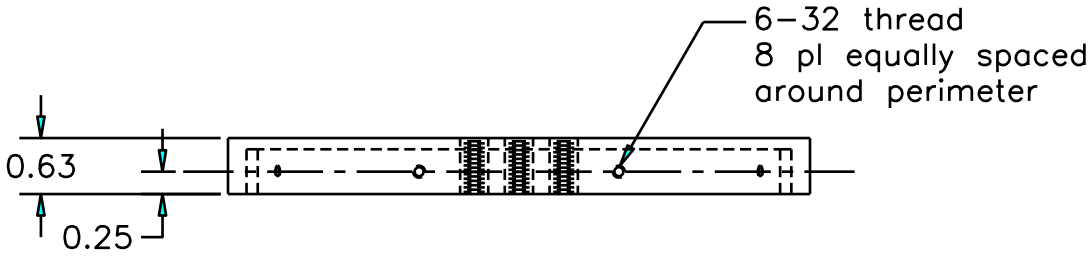

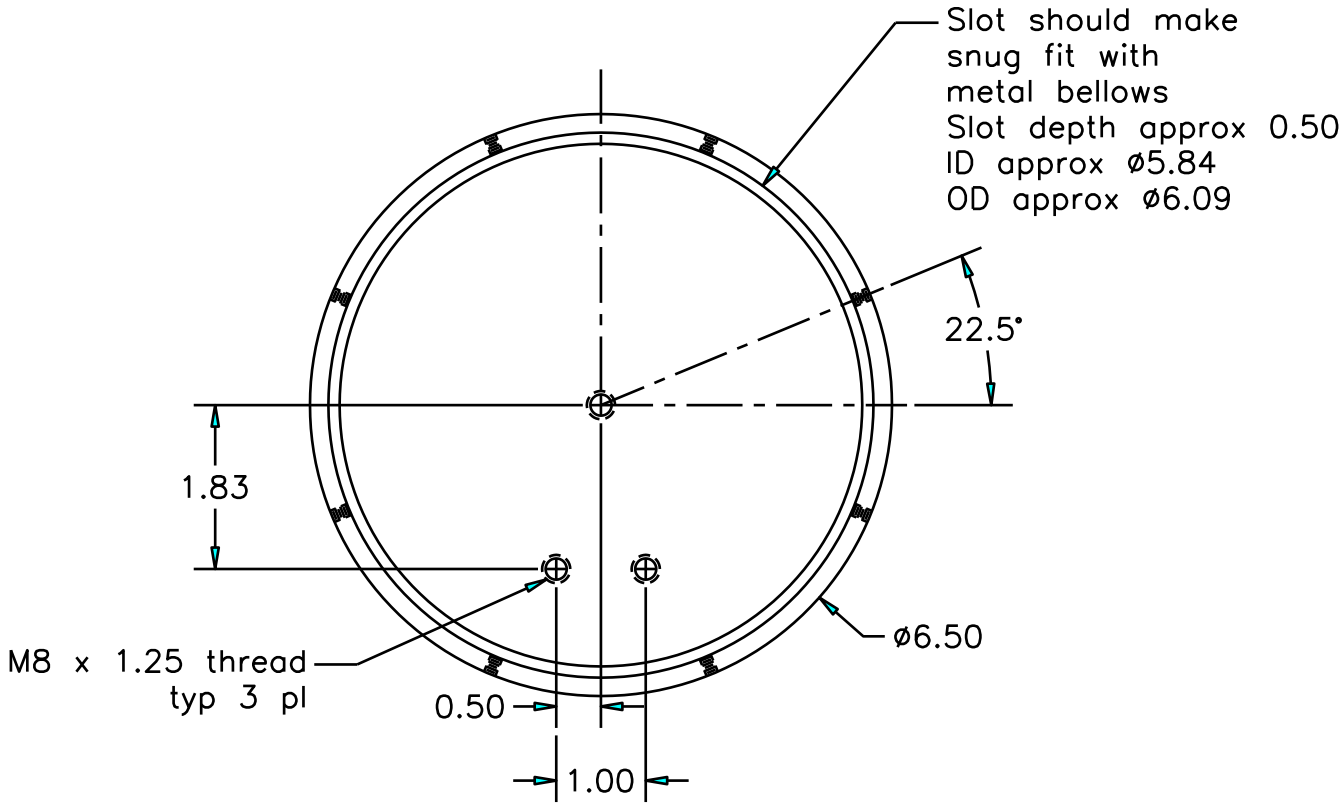

Notes:
1. Material 6061 Al
2. Finish anodize.
3. One required

Unless otherwise specified:
Dimensions are in inches
Break all edges 0.01 max
Remove all burrs
Tolerances are:
.XX ±.01 .XXX ±.005
Angles 0.5°
Fractional ±1/32

Cough sim bellows back.dwg

Rear end cap for bellows cough sim

Date: 2/22/2013

Drawn by: William G. Lindsley

Scale: 1/2

Sheet 1 of 1

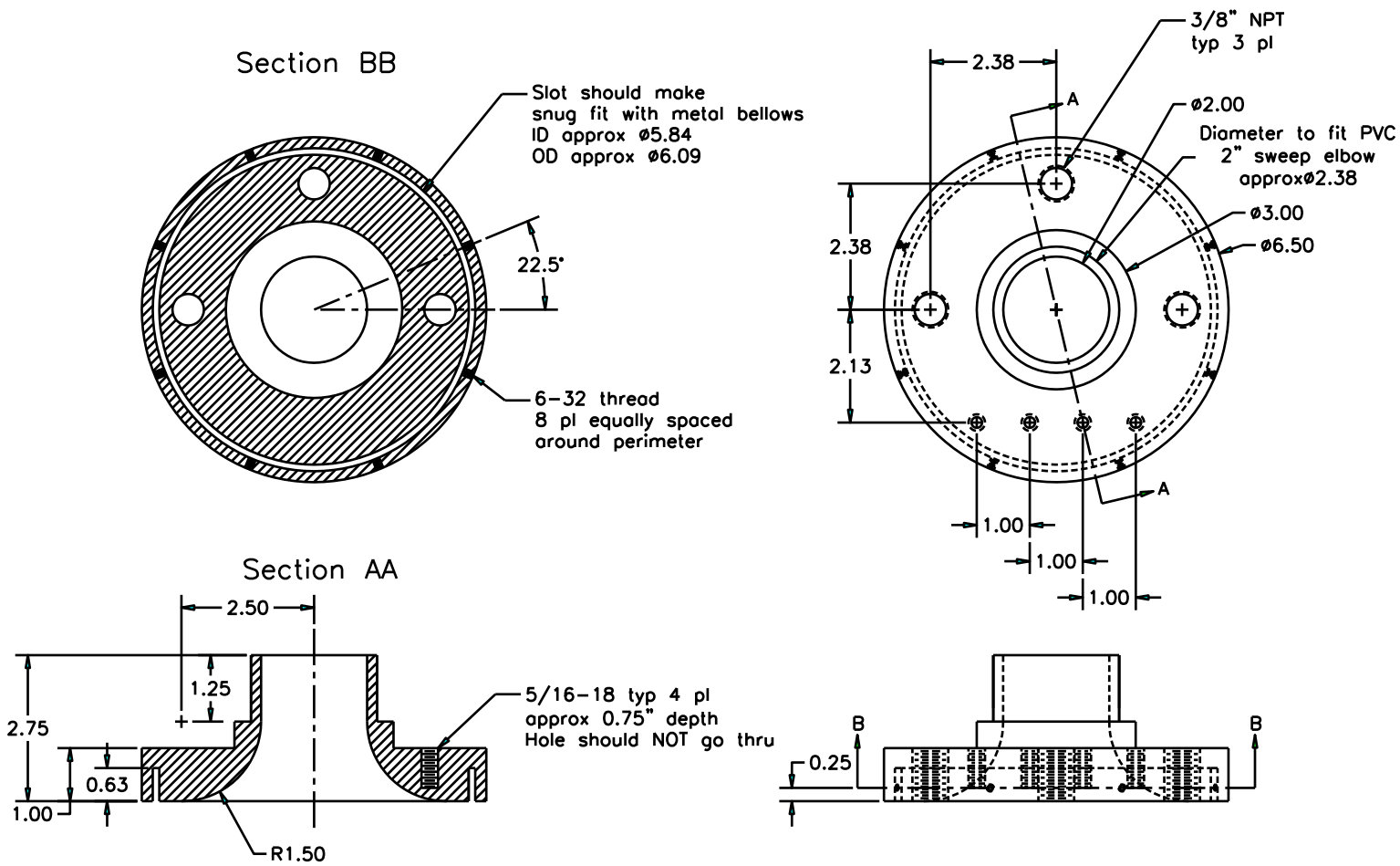

Notes:
1. Material 6061 Al
2. Finish anodize
3. One required

Unless otherwise specified:
Dimensions are in inches
Break all edges 0.01 max
Remove all burrs
Tolerances are:
.XX ±.01 .XXX ±.005
Angles 0.5°
Fractional ±1/32

Cough sim bellows front.dwg

Front end cap for bellows cough sim

Date: 2/22/2013

Drawn by: William G. Lindsley

Scale: 1/2

Sheet 1 of 1

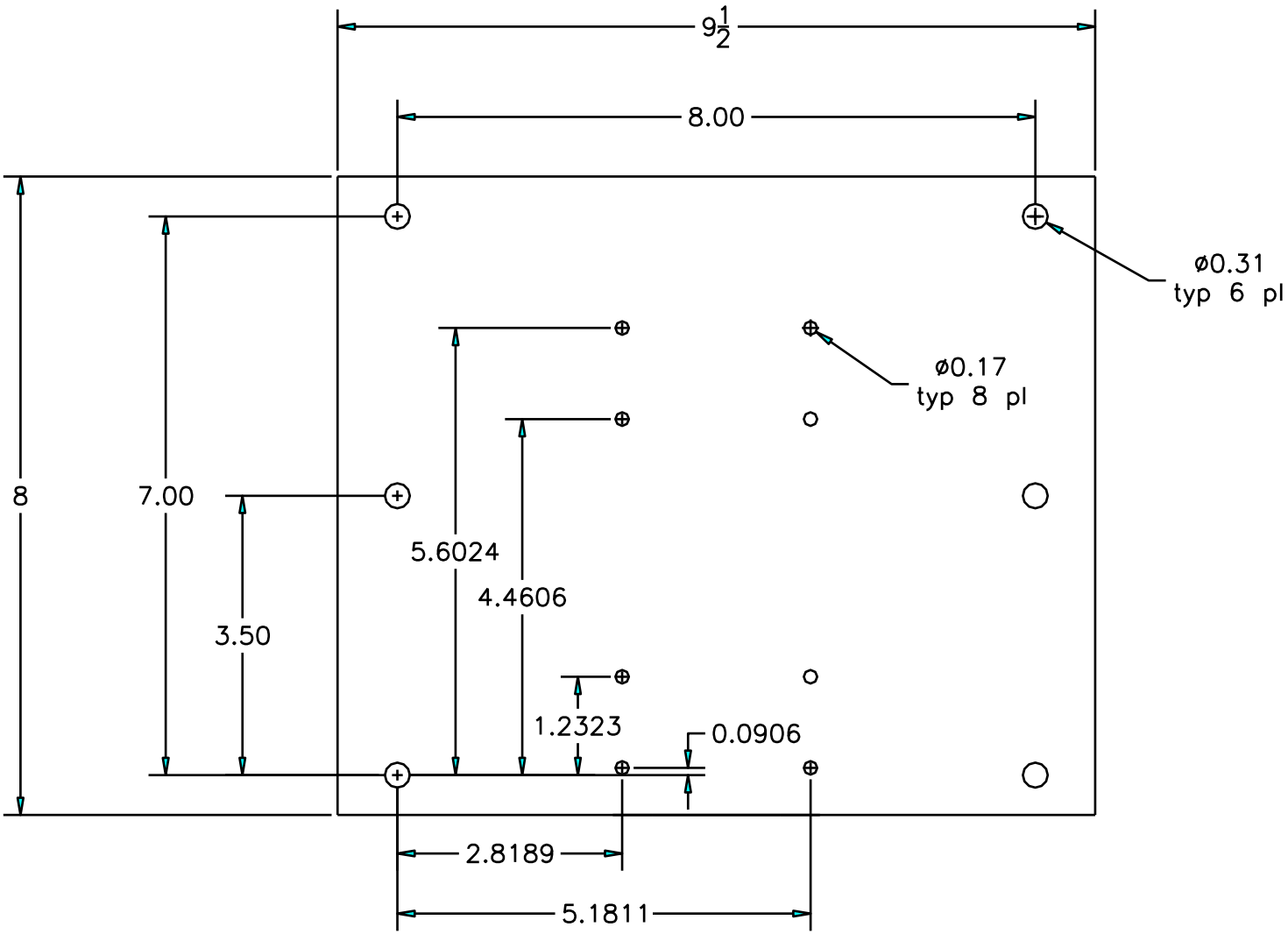

Notes
1. Material 6061 Al, 0.5" thickness
2. Finish anodize.
3. One required.

Linear motor mounting plate.dwg

Unless otherwise specified:
Dimensions are in inches
Break all edges 0.01 max
Remove all burrs
Tolerances are:
.XX ±.01 .XXX ±.005
Fraction 1/32 Angles 0.5°

Linear motor mounting plate

Date: 2/21/2013

Drawn by: William G. Lindsley

Scale: 1/2

Sheet 1 of 1

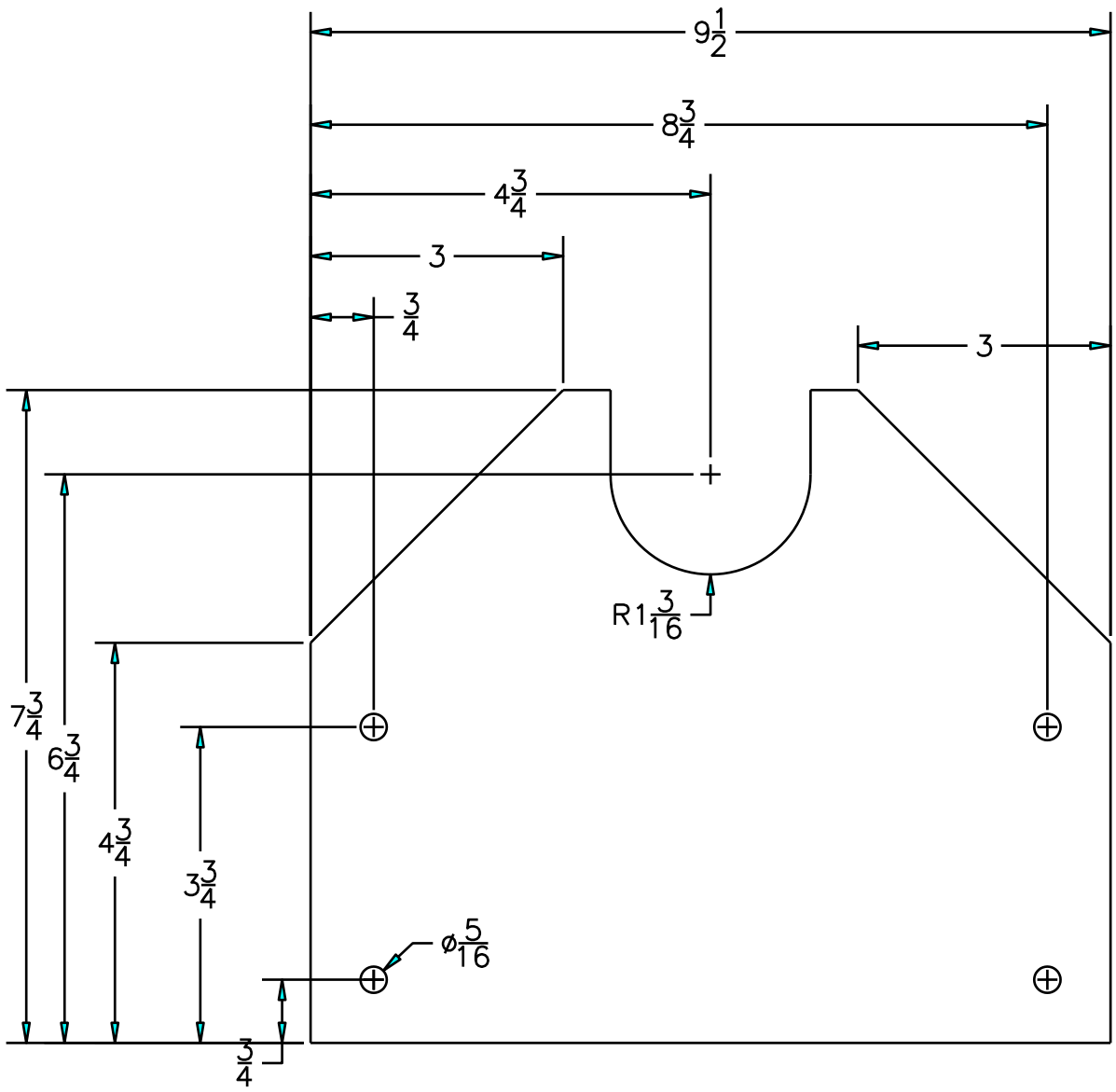

Notes:
1. Material ½" PVC

Unless otherwise specified:
Dimensions are in inches
Break all edges 0.01 max
Remove all burrs
Tolerances are:
.XX ±.01 .XXX ±.005
Angles 0.5°
Fractional ±1/32

PVC chamber front support plate

Date: 2/21/2013

Drawn by: William G. Lindsley

Scale: 1/2

Sheet 1 of 1

PVC chamber front support plate.dwg